Coordination Chemistry Reviews 255 (2011) 2727–2745

Contents lists available at ScienceDirect

Coordination Chemistry Reviews

journal homepage: www.elsevier.com/locate/ccr

Review

Metal binding calixarenes with potential biomimetic and biomedical applications

Daniel T. Schühle[a,1], Joop A. Peters[a,**], Jürgen Schatz[b,*]

[a] Department of Biotechnology, Biocatalysis and Organic Chemistry, Delft University of Technology, Julianalaan 136, 2628 BL Delft, The Netherlands
[b] Department of Chemistry and Pharmacy, University of Erlangen-Nürnberg, Henkestrasse 42, 91054 Erlangen, Germany

Contents

ARTICLE INFO

Article history:
Received 25 January 2011
Accepted 3 April 2011
Available online 14 April 2011

Keywords:
Calix[4]arene
Enzyme mimic
Artificial ion channel
Contrast agent

ABSTRACT

This article exploits the special geometry of calixarene derivatives and the resulting metal binding properties with a focus on biomedical applications. The use of calixarenes as mimics of ion channels through artificial cell membranes, as mimics of metalloenzymes, and in the promising emerging field of calixarene based agents for medical imaging and radiotherapy is summarized.

© 2011 Elsevier B.V. All rights reserved.

* Corresponding author. Tel.: +49 9131 8525766; fax: +49 9131 8524707.
** Corresponding author.
E-mail addresses: schuhle@nmr.mgh.harvard.edu (D.T. Schühle), j.a.peters@tudelft.nl (J.A. Peters), juergen.schatz@chemie.uni-erlangen.de (J. Schatz).
[1] Present address: A.A. Martinos Center for Biomedical Imaging, Harvard Medical School and Massachusetts General Hospital, 149, 13th Street, Suit 2301, Charlestown, MA 02129, USA.

0010-8545/$ – see front matter © 2011 Elsevier B.V. All rights reserved.
doi:10.1016/j.ccr.2011.04.005

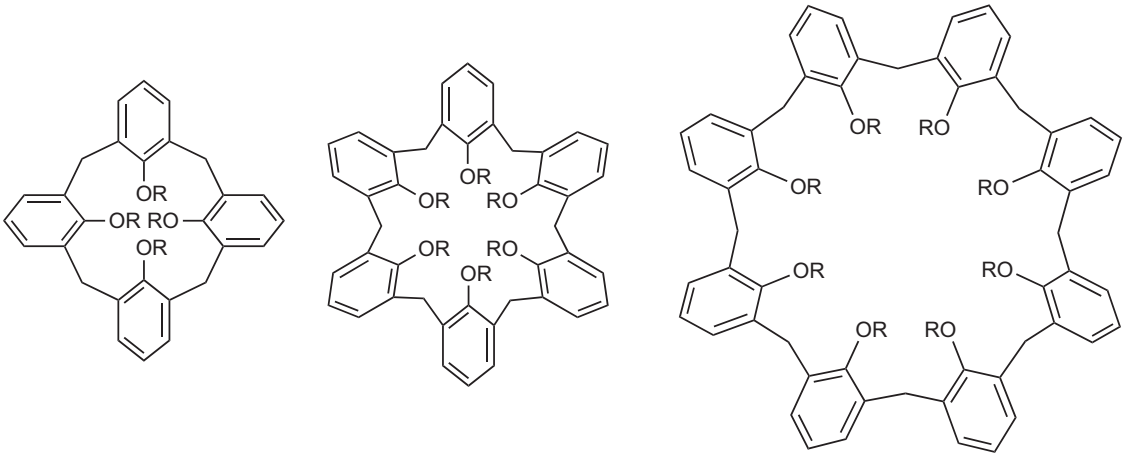

Fig. 1. The structures of calix[4,6 and 8]arenes [8].

1. Introduction

By virtue of their unique geometry, calixarenes (Fig. 1) are attractive for application in chemistry, physics, biology, medicine and in many interdisciplinary fields [1–11]. For example, David Gutsche selected calixarenes as rigid synthetic platforms in the design of an aldolase mimic and this lead him to his pioneering work on improved synthetic routes towards them [12].

At least 2*n* identical binding sites can be introduced in a calix[*n*]arene scaffold, whereas the hydrophobic cavity formed by its phenyl moieties offers an additional binding site for non-covalent binding of a substrate. The resulting geometric arrangement of the binding motifs within a single molecule can lead to multivalent binding and thus to the selective formation of highly stable aggregates [13]. Other small scaffolds such as benzene derivatives, cyclodextrins, monosaccharides, metal complexes, or azamacrocycles are often synthetically less easily accessible.

Molecules with completely different biological properties can be obtained simply by changing the conformation of the calixarene backbone as illustrated in Fig. 2 on calix[4]arenes. The larger calix[6 or 8]arenes are more mobile and can better adjust their conformation to a geometry that is required for efficient binding of a target/substrate in their cavity (induced fit). In this article, recent developments (since about 1999) in the biomedical chemistry of metal binding calixarenes are highlighted. Beautiful work on other biologically active calixarenes such as e.g. sulfonato calixarenes or hydrocarbon or peptide functionalized calixarenes further demonstrate the immense potential of this class of compounds. Since several excellent reviews on these studies exist already, they are not included in this manuscript [1–11,14]. Furthermore, thiacalixarenes, resorcinarenes and pyrogallolarenes are not included, because these compounds have a different coordination and redox chemistry.

2. Artificial ion channels and ion shuttles

The intra- and extracellular concentrations of physiologically relevant metal ions usually differ. The transport of inorganic cations between intra- and extracellular compartments occurs mainly through two mechanisms: (i) ionophore mediated transport by which a chelator binds the metal ion and transports it through the lipophilic cell membrane and (ii) formation of transmembrane channels with selectivity for a certain metal ion [15]. Whereas ion shuttles can transport cations with a rate of 10^4 ions per second, channels can transport ions about 10,000 times faster. As a result, there is considerably more interest in channels than in the development of new ionophores. In general, these channels provide a hydrophilic path inside the hydrophobic cell membrane. Malfunctioning of natural systems can lead to severe diseases. Therefore, better understanding of transport processes of metal cations across phospholipid bilayers is desirable. A major challenge is the design of model systems that do not only allow charged metal ions to pass a hydrophobic bilayer but that also show selectivity for a particular cation [15]. Especially systems that are able to transport the biologically most relevant alkali metal cations, Na^+ and K^+, selectively through membranes are of great interest. The ratio of the concentrations of Na^+ and K^+ in- and outside cells are important for e.g. the proper functioning of signal transduction in nerves.

Reported in 1955, macrocyclon, a calixarene derivative with *tert*-butyl or *tert*-octyl groups on the upper rim and polyethyleneglycol functions at the lower rim, has anti-tuberculous effects [16]. Nowadays, there is speculation that the anti-tuberculous and anti-inflammatory properties of these compounds might be due to their possible function as ion channels [17]. In general, suitable amphiphilic calixarenes can be incorporated into biological membranes and then serve as artificial ion channels [18–20]. This type of calixarene may also be used for selective binding of metal ions.

There are strong indications that, as a result of the size and the hydrophobicity of the calix[4]arene backbone, the potassium aquo ion is partly dehydrated prior to its transport through the cavity towards metal binding functions on the *lower rim* [15]. Natural ion channels have this dehydration capability as well and, consequently, this property is of importance for a successful mimic [15].

In principle, calixarenes can form ion channels through membranes in two different ways. Cone conformers are likely to form

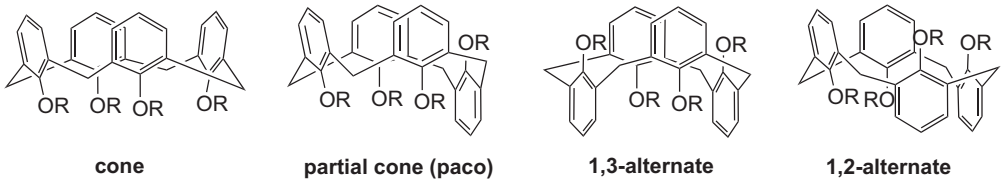

Fig. 2. The four possible conformations of calix[4]arenes [8].

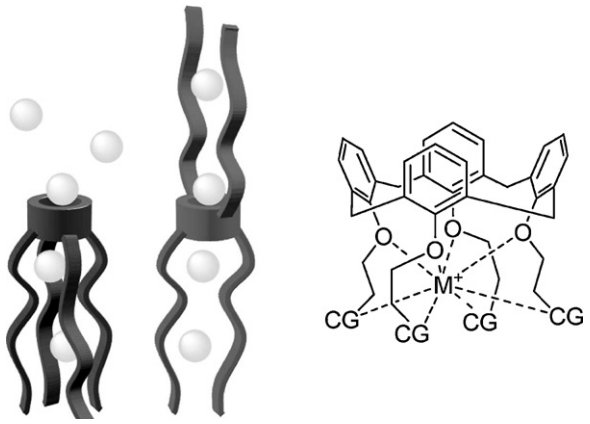

Fig. 3. Two possibilities of how calixarenes can span phospholipid bilayers (left, image reprinted with permission from Ref. [15]) and most common binding motif of calixarene based ion channels (right, CG = coordinating group).

channels with the cavity located at either the outer or the inner surface of the membranes whereas 1,3-alternate conformers probably form channels with the calixarene cavity located inside the membrane (see Fig. 3). The most promising ion channel mimics should have the potential to be included into lipophilic membranes and at the same time should provide binding sites for metal ions to allow the transport of charged species through the apolar cavity. Research on calixarene based artificial enzyme mimics is limited to Na^+ and K^+ transport so far, but systems that are able to transport other physiologically important cations such as Ca^{2+} or Mg^{2+} can be envisioned as well. Sulfinylamidine and *N*-chalconeamide functionalized calixarenes were already shown to influence Ca^{2+} transport by Mg^{2+}, ATP-dependent calcium pumps in rat uterus smooth muscle subcellular structures [21,22].

Calixarenes that cannot physically span the bilayer but can transport metal ions through the bilayer do not necessarily act as ion shuttles. They can self-assemble within the bilayer to form channels for ions in analogy to the naturally occurring gramicidin-like aggregates [15]. This makes the understanding of the mechanism of action of such ionophores difficult. In many of the examples discussed below, the ion transport mechanism is not known.

2.1. Na^+ channels

In a systematic study on the selectivity of the transport of alkali metal ions through a phospholipid bilayer model by calixarenes **1** of various sizes (from calix[4–8]arenes, Fig. 4), Jin et al. demonstrated that the tetramer ($n = 1$) leads to a permeability for Na^+ ions that is 20 times higher than that for all other metal ions tested [23]. Probably, this calixarene forms a dimer within the bilayer that is able to span the membrane thus allowing efficient Na^+ transport or it serves as an ion shuttle. The higher calixarenes of this type have some selectivity for larger alkali ions; compound **1** with $n = 3, 4$, and 5 show preference for K^+, Rb^+, and Cs^+, respectively [18].

In studies of the parameters determining the metal ion flux through artificial cell membranes, it may be useful to have a possibility to block this transport. For example, **2** [15] formed a photo-switchable artificial Na^+ channel which has a Na^+-selectivity similar to that of calix[4]arenes **1** ($n = 1$). Upon irradiation with UV-light (>310 nm) the anthroyl units dimerize and then block the way for diffusing metal ions. Upon switching off the UV-light, the dimer slowly falls apart and ion transport resumes.

The influence of different conformations of the calixarene backbone on the transport of protons and Na^+ ions through liposomes was investigated by inclusion of ionophores **3a–e** bearing cholic acid moieties (Fig. 5) into liposomal membranes [24]. The compounds with 1,3-alternate conformation (**3a–c**) are much more effective in ion transport than the corresponding compounds in *cone* conformation. This indicates that different transport mechanisms might be acting in compounds **3**. The authors rationalize that **3d** and **3e** form dimers in the membrane whereas the 1,3-alternate ionophores are able to span the bilayer providing a much better channel. Acylation of the steroid moieties has only a minor influence on the transport efficiency.

Triton (Fig. 6) is a well-known non-ionic surfactant that is widely used to destroy liposomes and cell membranes by penetrating the bilayers. This propensity was the inspiration to synthesize **4** [25]. However, **4** did not show any ion transport, but its calix[6]arene analogue bearing methylated phenolic groups is a good Na^+ transporter possibly due to a weaker binding of the metal and the resulting easier translocation of the metal ion through the hydrophilic channel provided by **4**. Alkali metal ion selectivities have not been reported for these systems.

Compound **5** showed negligible activity, which was ascribed to its inability to completely span the phospholipid bilayer [26]. Another reason could be that the long alkyl-spacers are not able to provide a hydrophilic channel through the lipid bilayer.

Alternatively to the size of the available cavity, the selectivity of calix[4]arenes for sodium ions can be controlled through the electron density on the chelating phenolic ether units. A decrease of electron density on donor groups leads to overall weaker binding but at the same time the selectivity for Na^+ over K^+ becomes up to 10 times higher (see Fig. 7) [27]. Compound **6** or derivatives were not

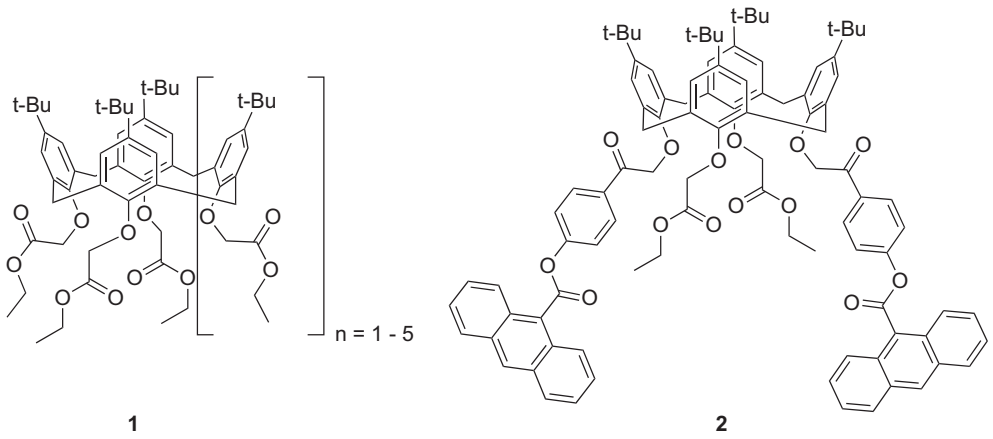

1 2

Fig. 4. Na^+ selective calixarenes [15,23].

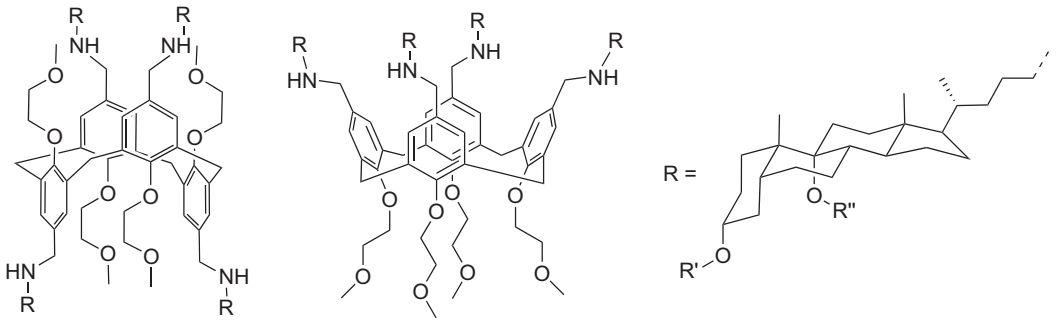

Fig. 5. Cholic acid containing ionophores **3a–e** [24].

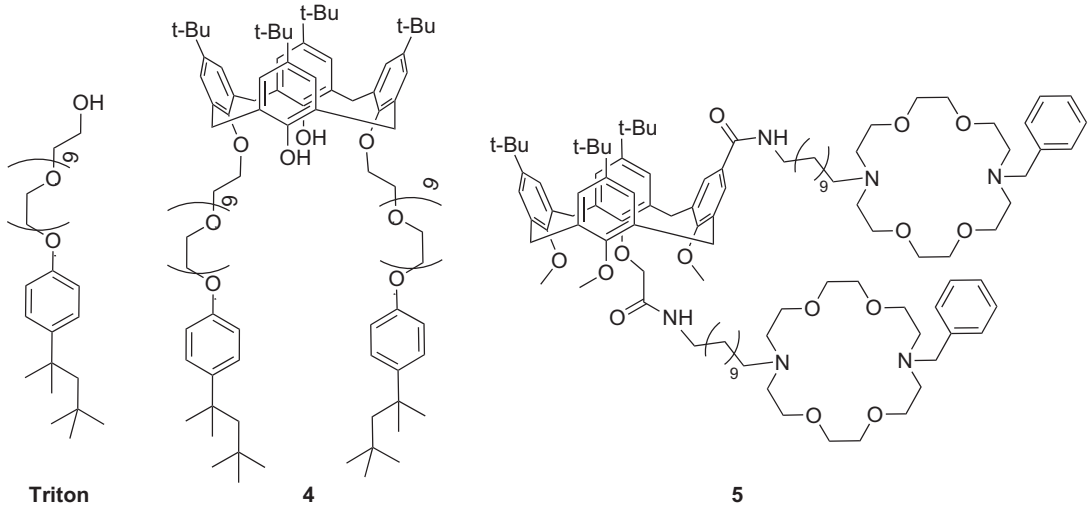

Fig. 6. Triton and calix[4]arene based ionophores [25,26].

evaluated as ion transporters yet but their high selectivity makes them attractive model structures for future investigations.

2.2. K^+ channels

Control of the Na^+/K^+ ratio inside artificial cells requires the presence of both Na^+ and K^+ channels. However, only a few reports on calixarene based selective K^+ ionophores have been published and only little is reported about K^+ transport through phospholipid bilayers. A promising mimic of K^+ transport was reported by Arduini et al., who showed that the tubular **8** (Fig. 8) forms channels with about the required length to span such a bilayer [28].

A four-fold symmetric arrangement of Thr-Val-Gly-Tyr-Gly polypeptides forms the selectivity filter of the K^+ channel in *Streptomyces lividans*. Compounds **9** are mimics of this system and were used to learn more about the mechanism of cation transport and about the origin of the selectivity of this system [29]. Initially, the K^+ ion is bounded by the phenolic and the valine carbonyl oxygen atoms of all compounds studied. Hydrogen bonding was crucial in this system: for the tripeptide, the N_{val}-H···O=C_{val} bonds are much stronger than for the shorter peptides. This effect stabilizes this species and as a result the metal binding is relatively weak. This might facilitate the release of the ion and therefore, the ion translocation.

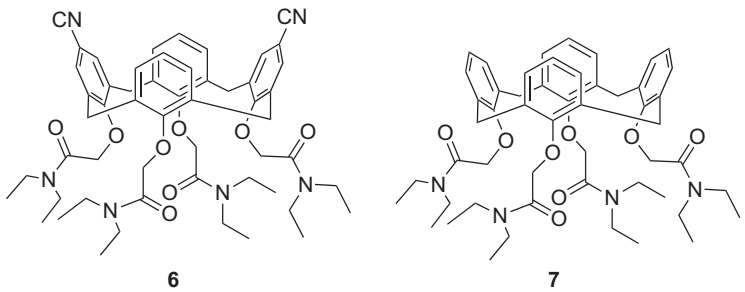

Fig. 7. Calix[4]arene **6** has 10.2 times higher selectivity for Na^+ over K^+ compared to its parent derivative **7** [27].

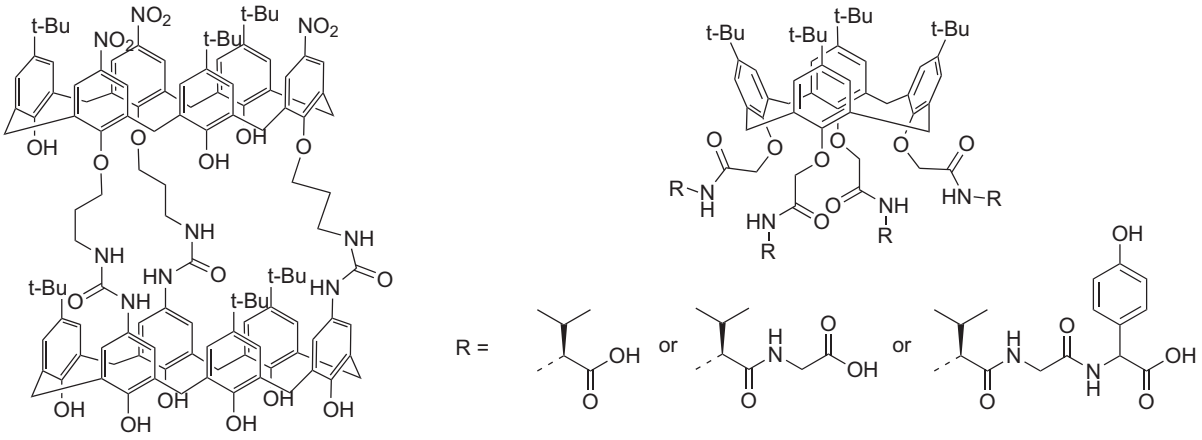

8 9

Fig. 8. Synthetic K^+ channels [28,29].

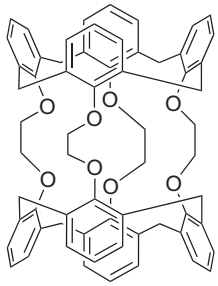

10

Fig. 9. A K^+ selective calix[4]arene dimer [30].

Beer and co-workers reported that another possibility to span the bilayer by calix[4]arene dimers is with compounds similar to **10** (Fig. 9) with interconnected *lower rims* [30]. It may be expected that elongation of the bridges between the calixarene units of **10** with, for example, ethylene glycol moieties, may provide a channel for K^+ cation transportation that spans the bilayer but the synthesis of such a dimer is a challenge.

3. Metalloenzyme mimics

Enzymes are amongst the most selective catalysts available. Their active sites provide a variety of non-covalent interactions with substrates that control the recognition process and, therefore, the selectivity of the enzyme. These include hydrogen bonding, charge/charge, CH/π and cation/π interactions. Many enzymes contain metal ions that play a key role in the structural organization of the peptide, in the recognition processes of substrates or as the catalytic centers in the active site. In the latter case, the enzyme does not only act as a very large ligand with preorganized metal binding sites, but it also provides a cavity and a corridor to control the access of the substrate and, therefore, selectivity and reactivity of the metal ion site [1]. Enzymes are complex systems that are not easy to study. Therefore, simpler low molecular weight model systems are used to gain insight into the action of enzymes. Accordingly, there is still a need for good mimics that can be characterized simpler than the parent enzymes. Supramolecular approaches to enzyme mimics are of special value because the complex nature of enzymes can be mimicked without too much synthetic effort [31]. It is not surprising that calixarenes find applications in metal-based catalysis of standard organic transformations [32] and as building blocks for such metalloenzyme mimics. Calixarenes can easily be functionalized and in addition offer a platform to prearrange chelating groups or bound metal ions in a three-dimensional space. Furthermore, calixarenes can adopt different conformations (induced fit or dynamic preorganization) and can coordinate other molecules to mimic hydrophobic pockets of enzymes [1].

3.1. Calix[4]arenes

3.1.1. Zn^{2+}-based phosphodiesterase and lipase mimics

Many metal containing phosphodiesterases use one, two or three divalent metal centers such as Zn^{2+} for the activation of the substrate [33,34]. The prearrangement of metal centers using synthetic spacers is crucial in mimics of such enzymes since tetrahedrally coordinated Zn^{2+} centers are assumed to activate the phosphate group and a nucleophilic water molecule, to stabilize the pentacoordinate phosphorus transition state and possibly the leaving group by cooperative action (Fig. 10) [35]. In studies of

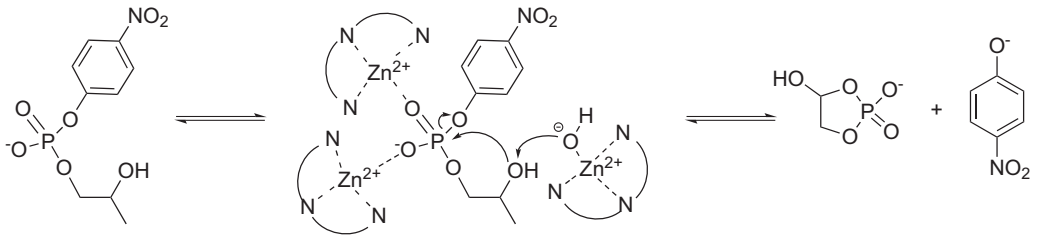

Fig. 10. Possible mechanism for HPNP cleavage by trinuclear phosphatase models [35].

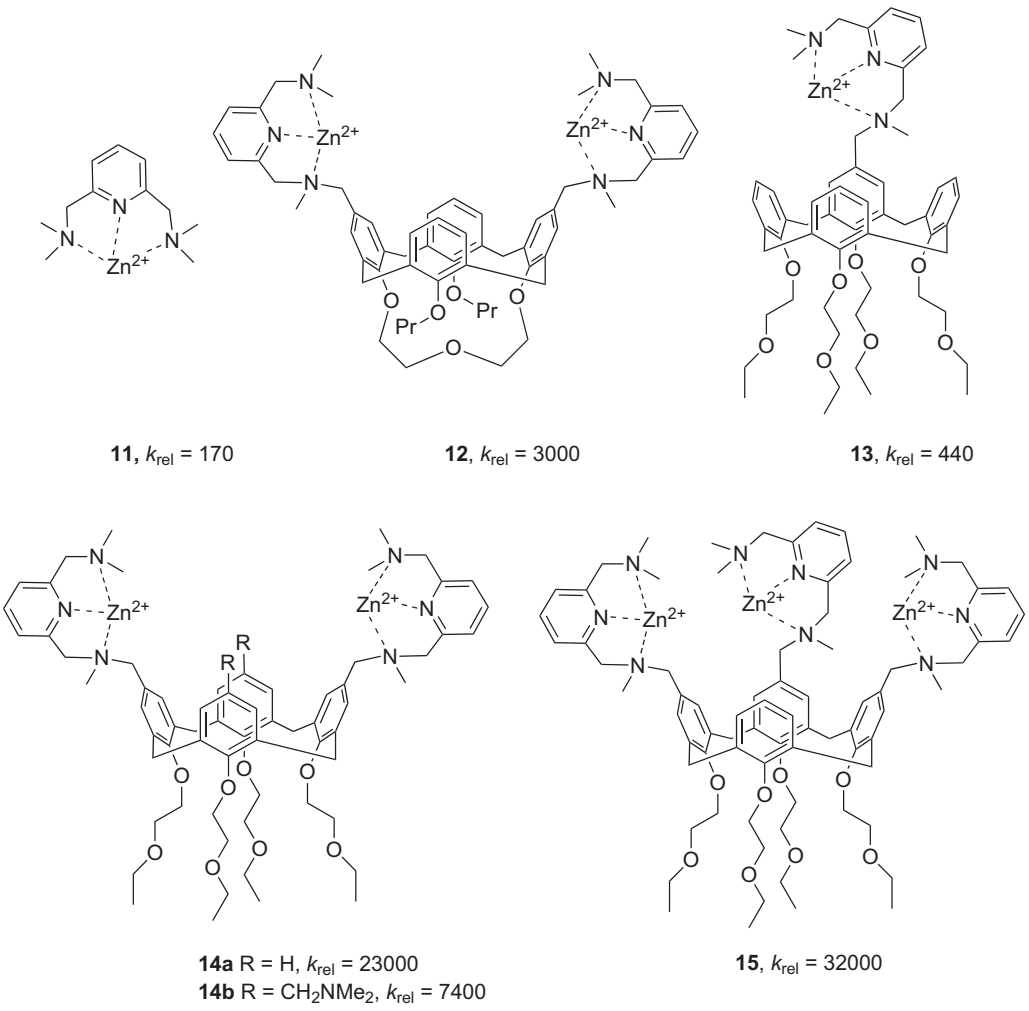

Fig. 11. Mono-, di- and trinuclear Zn(II) phosphatase mimics and relative rate acceleration factors k_{rel} [33–35].

phosphatase activity, 2-hydroxypropyl-p-nitrophenyl phosphate (HPNP, Fig. 10) is used as RNA model substrate, the intramolecular cyclization reaction, and the release of p-nitrophenolate being the driving force of the reaction. Reinhoudt and co-workers investigated the performance of calix[4]arenes **12–15** as enzyme mimics (Fig. 11). Although Zn^{2+} is chelated by non-natural chelating units and the catalysis was performed in a MeCN/aqueous buffer mixture, the results gave information on the mode of action of corresponding enzymes (Fig. 10). The particular chelating units applied were selected because they are easily accessible and are able to complex a variety of divalent transition metal ions [34].

Relative rate acceleration factors k_{rel}, defined as the ratio of the observed rate constant of the reaction in the presence of the catalyst and the rate constant of the non-catalyzed reaction, can be used to directly compare the activity of catalysts. The parent system **11** has a much lower catalytic activity than its mononuclear calixarene based conjugate **13**. This indicates that the calixarene backbone is involved in the catalysis, probably by binding the substrate inside the hydrophobic pocket [35]. The dinuclear complex **14a** shows a rate acceleration of 23,000 in the transesterification of HPNP over the non-catalyzed reaction, whereas the mononuclear **13** analogue is 50 times less active. This suggests that the metal centers have cooperative action and that the hydrophobic cavity is involved in the binding of the substrate. On the basis of extensive kinetic studies, the high catalytic activity of **14a** was ascribed to the high affinity of the substrate to the binding site. The rate of conversion was moderate, the high catalytic activity being a consequence of the high stability of the intermediate Michaelis–Menten like substrate/receptor complex. The mechanism is analogous to that depicted in Fig. 10, but now the phosphate function is bound by a single metal ion. The more rigid calix crown model compound **12** exhibits a lower substrate affinity and a lower catalytic activity than the conformationally less restricted **14a**, which demonstrates the need for some flexibility within the calixarene to enable cooperative effects between the metal centers (induced fit). The trinuclear complex **15** induces a rate acceleration of 32,000 compared to the uncatalyzed reaction, which is rationalized by the activation of the nucleophile (water) by the third metal center (see Fig. 10). Compound **16**, the vicinal analogue of **14a**, has a lower activity probably due to weaker binding of the substrate (Fig. 12) [36]. In a later study, it was observed that a trinuclear complex similar to **15**, but now with two Zn^{2+} and one Cu^{2+} ions, accelerates the reaction even more and shows high selectivities for certain RNA nucleotides [37]. Probably, this is caused by the synergy of the metal ions: Zn^{2+} leads to good substrate binding, Cu^{2+} to high conversion.

Comparison with the natural system, where basic histidine units often support the catalysis by providing hydroxide ions, led to the development of **14b** [33]. Rather than activation of water by a third metal ion in the form of a hydroxo complex, hydroxide is generated by one of the tertiary amine groups in proximity of the bound substrate. The decrease in catalytic activity with respect to **14a** is caused by the weaker binding of HPNP due to the partially blocked access to the hydrophobic cavity as well as to a slower conversion, which can be ascribed to a less favorable binding geometry

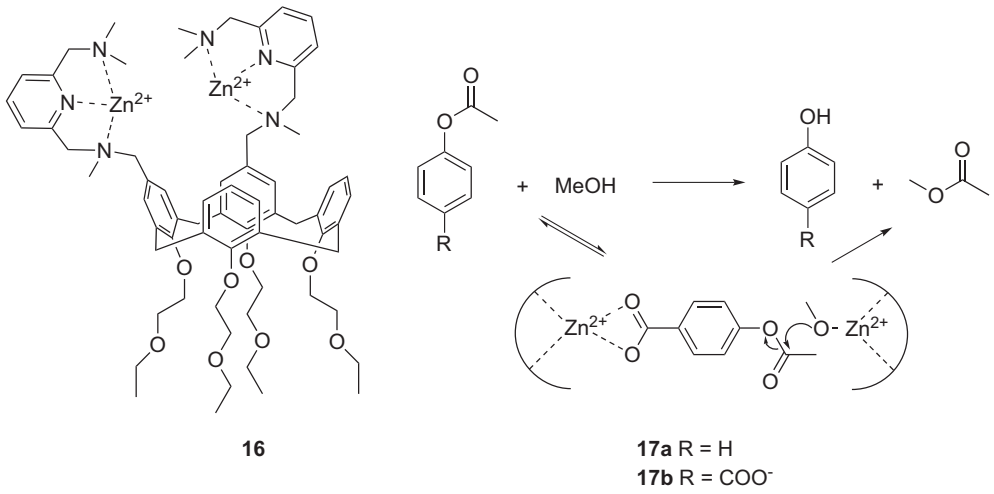

Fig. 12. Vicinal Zn^{2+} complex **16** and solvolysis reaction tested [36].

of the substrate. Both facts can be explained by the steric demands of the dimethylamino groups that hamper the binding of the substrate and, therefore, the simultaneous binding of HPNP to both Zn-centers.

The ability of complexes **11**, **14a**, **15** and **16** to cleave carboxylic acid esters was investigated by solvolysis experiments in methanol (Fig. 12) [36]. Potentiometric titrations performed on model compound **11** showed that the complex behaves as a weak acid with a pK_a of 9.5 which corresponds to the deprotonation of a Zn^{2+} bound methanol molecule. This implies that for the di- and trimetallic Zn-complexes, one Zn-unit binds a solvent molecule as its methoxide whereas the second one is able to bind **17b** via its COO^- function (see Fig. 12). As a result, in binuclear complexes, one metal ion preorganizes the substrate for the nucleophilic attack of the activated solvent molecule that is provided by the other metal. At the same time, the binding of the carboxylate by the Zn^{2+} center activates the substrate for nucleophilic attack by the electron withdrawing effect of the metal ion. With **17a** as the substrate, the conversion is much

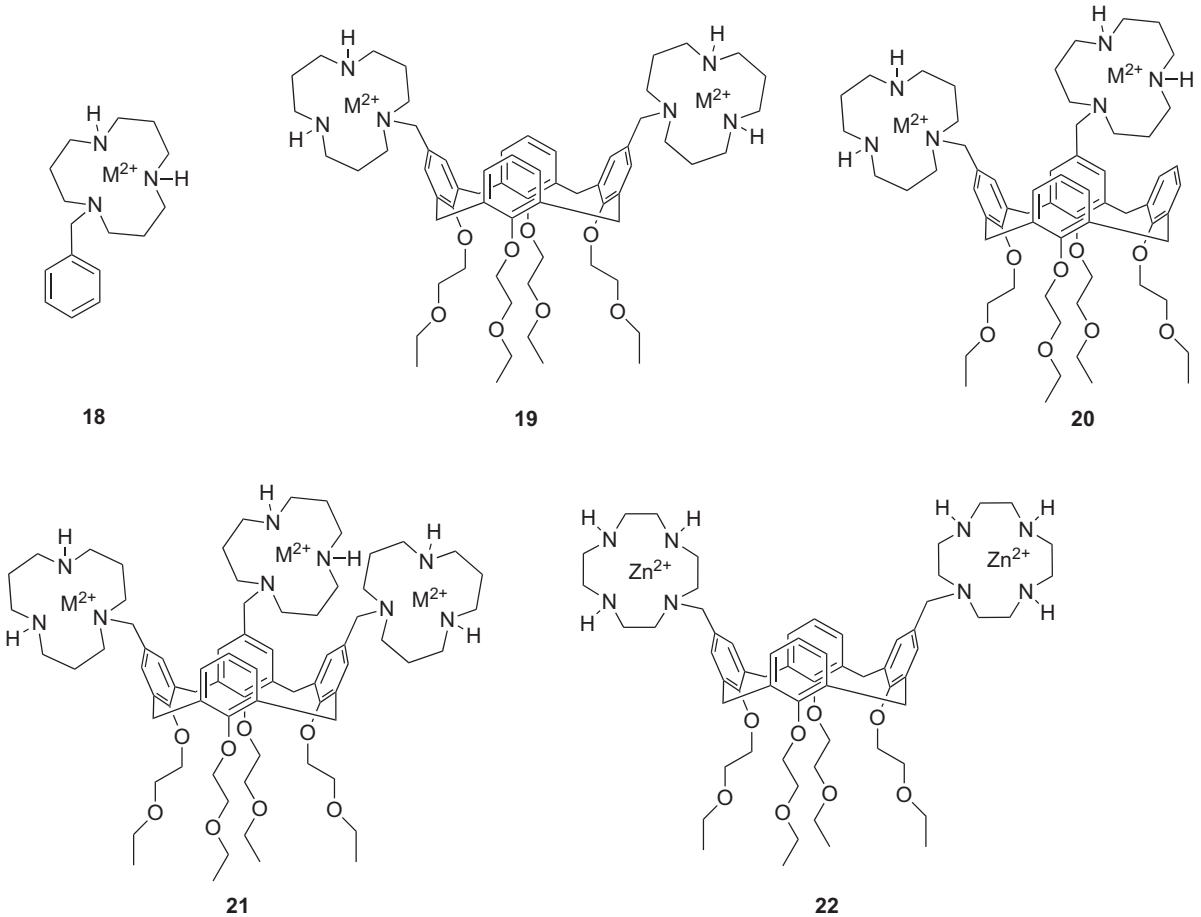

Fig. 13. Azacrown ether based metalloenzyme mimics [40–42].

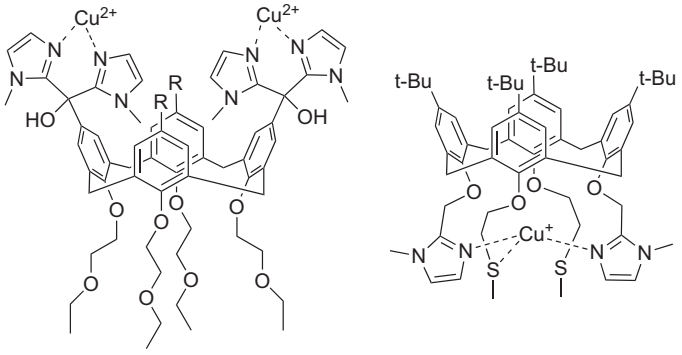

23a R = H
23b R = CH_2OH
23c R = CH_2NH_2

24

Fig. 14. Bisimidazolyl-Cu-calixarenes [44,45].

slower; the lack of a carboxylate group leads to less efficient binding to the catalyst. Interestingly, and opposite to what was found in the studies with HPNP, the vicinal Zn_2-**16** is catalytically much more active than the corresponding geminal Zn_2-**14a** isomer. The relatively high activity of the vicinal isomer in this case may be caused by either better substrate binding or different conformation or hydration of the catalyst due the use of a different solvent system (MeCN/buffer for transesterification of HPNP and methanol for methanolysis). The general superiority of vicinal compared to geminal isomers in the solvolysis of phenol esters was supported in a later study [38]. Similar pyridine based calixarenes have been proposed as metalloenzyme mimics but no experimental evidence has been given [39].

Various azacrown ethers attached to the *upper rim* of calix[4]arenes were used to chelate Zn^{2+} [40]. 1,5,9-triazacyclododecane has three binding sites for metal coordination and, therefore, is favorable for tetrahedral coordination of Zn^{2+}. Since the mononuclear analogue was not soluble in the solvent applied (MeCN/aqueous buffer pH 7), compound **18** was chosen as a mononuclear reference. These compounds showed only low catalytic activities in the cleavage of HPNP. Since the activities of the bimetallic complexes **19** and **20** (after correction for the different metal concentrations) are not much superior to those of the monomeric **18**, it can be concluded that there is lack of cooperation between the metal centers and that the calixarene core has no significant effect. Nonetheless, these complexes catalyze the solvolysis of various phenol esters by methanol efficiently [41]. As for the dimetallic complex **16**, one Zn^{2+} binds a methoxide, which can act as a nucleophile in the solvolysis reaction of the coordinated substrate (see Fig. 12). Phenol esters containing carboxylate functions were again good substrates since they provide a binding site for the second metal center and are activated upon binding to the metal (see above).

The strong chelator 1,4,7,10-tetraazacyclododecane (cyclen) complexes Zn^{2+} resulting in a rigid and bulky substituent attached to the calixarene core [42]. The steric demands of the two chelates in **22** hamper the binding of the substrate and reduce the catalytic activity very dramatically. By contrast to the systems described above, the mononuclear analogue shows superior catalytic activity over the dinuclear **22** due to the reduced steric hindrance.

3.1.2. Cu^{2+}-based phosphatase mimics

The Cu^{2+} complexes of ligands **19**, **20** and **21** (Fig. 13) are sufficiently soluble in water to study transesterification without the need of organic co-solvents. Although these complexes are less active than their Zn-analogues, they have the advantage over other Cu^{2+}-based enzyme mimics that there is no dimerization of the copper centers leading to catalytically inactive species [40]. Model reactions with HPNP revealed that there is no cooperative action of the distally arranged Cu-atoms in **19** but a strong synergistic effect in the vicinal isomer **20**. The trimetallic **21** shows slightly less catalytic activity than **20**, which indicates that two vicinal copper centers perform the catalysis, whereas the binding of the substrate is slightly hampered by the third chelate. Especially the trimetallic Cu_3-**21** catalyst shows remarkable selectivity for certain diribonucleoside-2′,3′-monophosphates, which represent better models for RNA than HPNP and which allow detection of specific cleavage, if any. These compounds appeared also to be very selective in the phosphodiester cleavage of single-stranded RNA oligonucleotides [43]. The catalyst is highly efficient under close to physiological conditions and resembles the natural RNAses A in their selectivity.

Attempts to mimic metal enzymes more closely using methylimidazole as histidine analogue showed successfully that a cooperative effect of functional groups attached adjacent to the

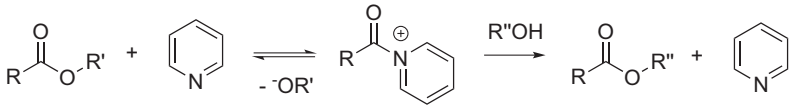

Fig. 15. Double displacement mechanism using pyridine as a catalyst.

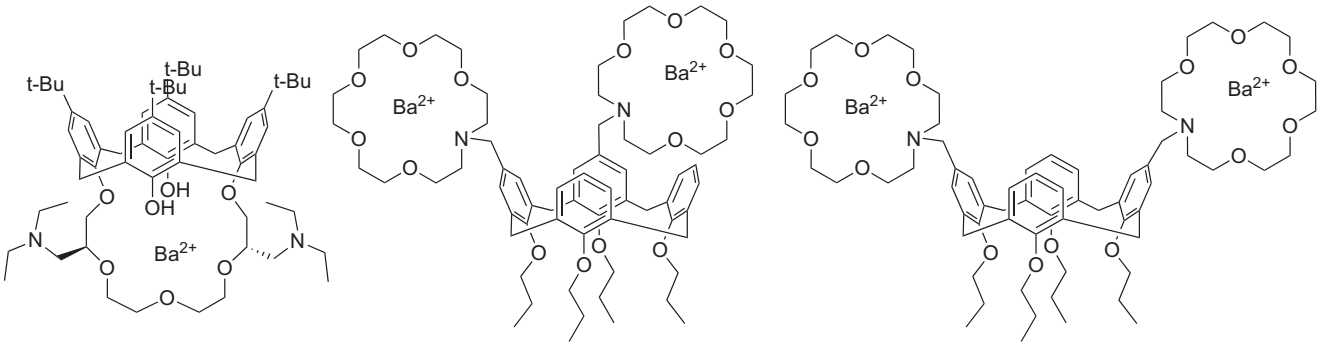

25 **26** **27**

Fig. 16. Ba^{2+} containing artificial acyl-transferase **25** and acylases **26–27** [46,47].

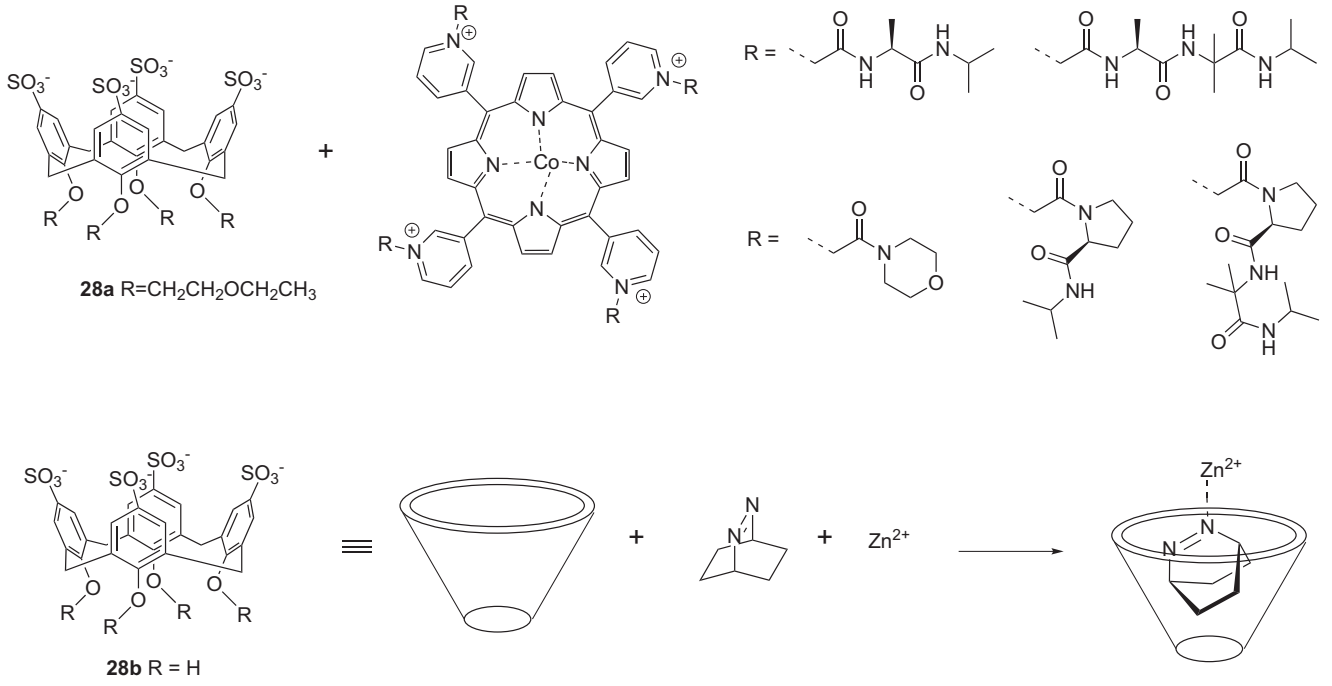

Fig. 17. Self-assembling metalloenzyme mimics [49,50].

metal centers can play an important role in catalysis (Fig. 14) [44]. The general mechanism is similar to that shown in Fig. 10, the difference being that the hydroxide is not provided by a third metal center but by a catalytically active Cu^{2+}-center. When the amino function in **23c** (Fig. 14) is protonated, it can assist in the binding and stabilization of the transition state. The corresponding Zn^{2+}-**23c** shows poor catalytic activity.

3.1.3. *Mimics for Cu^{+} containing enzymes*

In the reduced type 1 site (T1PR) in human ceruloplasmin, a permanently reduced Cu^{+} is bound close to the active site although it probably does not participate in any catalysis [41]. To elucidate the role of the metal center, the binding environment of the metal was mimicked by attaching two histidine analogues and two cysteine or methionine molecules to the *lower rim* of calixarene **24** (Fig. 14). The metal is complexed by two imidazoles and one sulfur atom leaving one coordination site for a potential substrate. Unfortunately, apart from some structural details, no further information on the performance of this compound as enzyme mimic was provided [45]. Nevertheless, the fact that the metal is oxygen stable is very promising for future investigations.

3.1.4. *Ba^{2+} complexes as acylase mimics*

Many enzyme catalyzed transacylation reactions proceed via a double displacement mechanism. First, an acylated enzyme intermediate is generated, which then acts as acylation agent for the nucleophilic substrate [46]. This principle is well-known in organic chemistry, for example from the pyridine catalyzed esterification of activated carboxylic acids (Fig. 15).

In such reactions, first pyridine reacts with the acylation agent creating a highly active species that subsequently transfers the acyl group to an attacking nucleophile. In mimics, the challenge is to

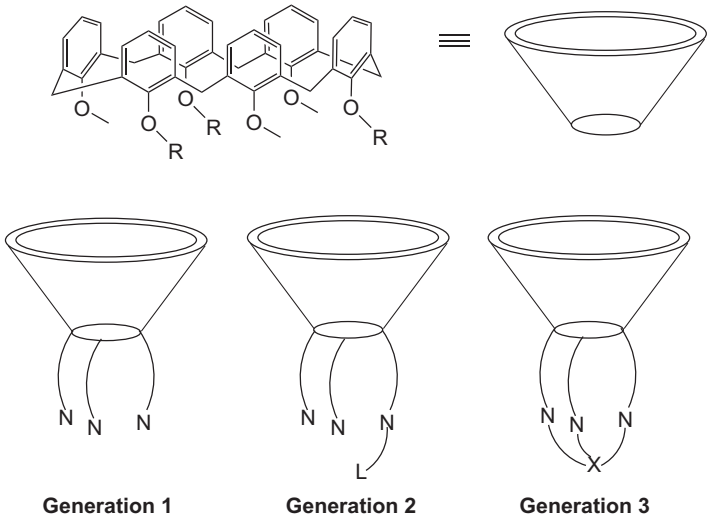

Fig. 18. The three generations of calix[6]arene funnel complexes.

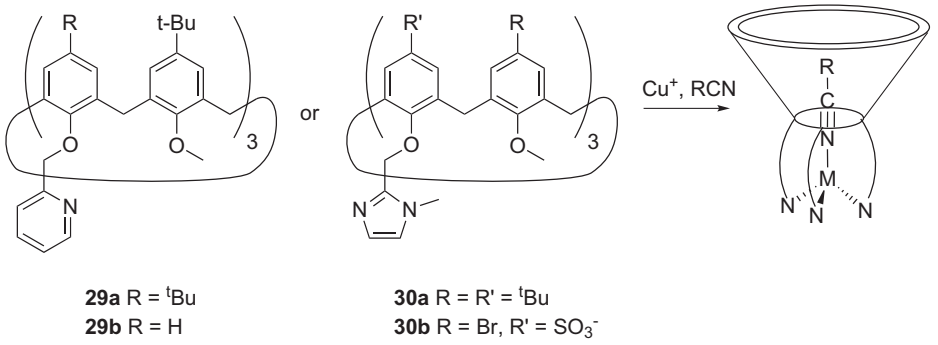

29a R = ^{t}Bu
29b R = H

30a R = R' = ^{t}Bu
30b R = Br, R' = SO_3^-

Fig. 19. Pyridine and imidazole based Cu^+ funnel complexes of the first generation [56,57].

achieve efficient transfer of the activated acyl to the nucleophile. This can be realized by using phenolic alcoholates, which are better leaving groups than alkoxides. In calixarene **25**, the phenolic groups can thus act as acyl-acceptors/acyl-donors, whereas the complexed Ba^{2+} acts as activating Lewis acid. The protonated amino groups function as intramolecular proton donor for the leaving group (phenolate) that is released in the first acylation reaction. In comparison to derivatives that do not contain the amino functionalities, **25** does not show better catalytic activity, which was ascribed to the steric demands of the diethylamino groups.

In a later study, two Ba^{2+}-ions were bound by crown ether moieties on the *upper rim* of calixarenes **26** and **27** (Fig. 16) [47]. Ethanolysis studies of various phenol esters indicated that the distance between the metal ions determines the substrate specificity of the catalyst. A similar reaction mechanism as depicted in Fig. 10 might also be operative in these reactions.

3.1.5. Self-assembling supramolecular enzyme mimics

Many natural enzymes consist of several self-aggregated subunits. Therefore, a general interest exists in combining several building blocks to artificial assemblies with properties that neither of the individual components has. Some examples demonstrate that calixarenes can be very useful in the design of such aggregates. These examples are based on the water soluble p-sulfonato calixarenes that were shown to interact with a range of metal ions before [48]. A supramolecular heme mimic was obtained by formation of a complex between p-sulfonato calixarene **28a** and porphyrins (Fig. 17) [49]. Thanks to strong charge/charge interactions association constants are as high as 10^5 M^{-1} in water, whereas the amide side chains provide sufficient water solubility. The formation of ternary complexes with nitrogen containing compounds depends on the size of the base. Small bases like 4-methylpyridine are bound inside the cavity spanned between calixarene and porphyrin, whereas larger molecules like caffeine are bound on the surface of the assembly. The self-assembled Co^{2+} complex shows a modest but significant facilitated O_2-transport through membranes due to the reversible binding of oxygen to the complex.

Nau and coworkers described the construction of enzyme mimics by dynamic self-assembly of p-sulfonato calix[4]arene **28b** with an organic guest and a divalent metal ion. The resulting system shows cooperativity in the binding (host-assisted metal–ligand bond formation) [50], demonstrating that the apolar guest provides an additional binding site for the metal, which stabilizes its interaction with the ligand. This proof of concept might lead to the development of a new generation of metalloenzyme mimics.

3.2. Calix[6]arenes

Enzyme mimics based on the calix[4]arene core are, as shown above, very suitable to study the effects of multinuclearity, the distance between the metal ions, and the flexibility of the linker on catalytic activity and selectivity. For monometallic enzymes, calix[6]arenes are better platforms since they do not only allow the binding of the metal in a polydentate way, but they also provide a hydrophobic channel that is similar to the hydrophobic pockets in the active sites of enzymes [1]. Calix[6]arenes are less rigid than calix[4]arenes and much more difficult to freeze in a particular conformation. On the other hand, they possess six phenolic oxygen atoms that can be functionalized in a defined way and they have a hydrophobic cavity that is larger than that in calix[4]arenes, which thus enables the complexation of larger guests. Calix[6]arenes can be methylated at three distal positions leaving the three remaining positions for the attachment of chelating groups. Therefore, tetrahedral metal ions with coordination number four are ideal candidates to be complexed because they can be bound very efficiently while still exhibiting one free binding site for e.g. substrate binding. Studies on calix[6]arene based enzyme mimics are so far focused on the binding of the metal, its influence on the complexation of a guest, its redox chemistry as well as on the influence of modifications on the calixarene core on those properties.

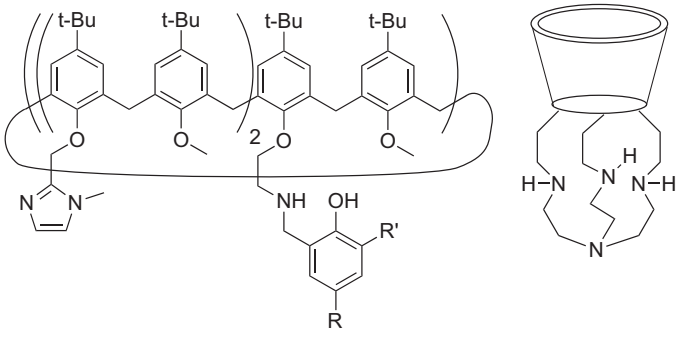

31a R = NO_2, R' = H
31b R = R' = ^{t}Bu

32

Fig. 20. Second and third generation ligands [64,65].

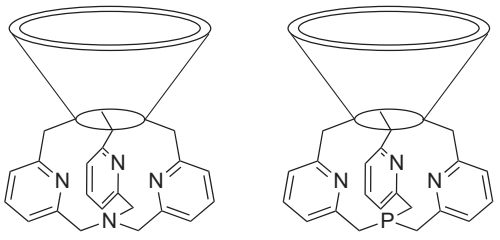

33 **34**

Fig. 21. Pyridine based third generation ligands [70,72].

Calix[6]arene based enzyme mimics, the so-called funnel complexes or calix-zymes, can be divided in three generations (Fig. 18) [1]. A way to fix the calix[6]arene platform in the *cone* conformation that is best suited for metal and guest complexation is by the complexation itself. First generation ligands were designed for this purpose and allowed detailed investigations of coordination chemistry, substrate binding and redox activity of the metal [51]. A second generation provides an additional binding site for metal complexation at the *lower rim*. These ligands are able to complex divalent metal ions more efficiently than the first generation, blocking possible dimerization and substrate binding outside the cavity. Furthermore, they provide the possibility to attach redox active ligands that are important in controlling the redox behavior of the bound metal.

The most prominent limitations of the two first generations of complexes are the relatively weak binding of the metal ions due to the flexible calixarene core and the long distances between the donor atoms [1]. Furthermore, oligonuclear species can be formed in the presence of, for example, bridging anions. In third generation ligands, the calix[6]arene azacryptands, the donor sites are interconnected by a fourth coordinating atom, which locks the calixarene core in the *cone* conformation.

3.2.1. Cu^{+}/Cu^{2+}-metalloprotein mimics

The pyridine based ligands **29** (Fig. 19) show poor binding of Zn^{2+} but are very good ligands for Cu^{+} [1]. The steric protection of the metal centers and coordination of a nitrile guest stabilize Cu^{+} in this low oxidation state thus avoiding the oxidation to Cu^{2+} by molecular oxygen and the dimerization of the metal ions [52]. The Cu^{+} ion is tetrahedrally coordinated by the three pyridine units and e.g. a solvent molecule inside the cavity in a bicapped trigonal pyramidal coordination geometry [53]. The redox potential from Cu^{+} to Cu^{2+} as well as the substrate binding is controlled by the ligand [54]. Due to the transmission of the chiral coordination geometry to the calixarene backbone, Cu^{+}-**29** exists as two different helical enantiomers at lower temperatures [55]. Effects of *upper rim* substitution on the binding and exchange of guest molecules (MeCN, PhCN) were investigated using **29a** and **29b** [56]. The steric demands of the six *tert*-butyl groups in **29a** lead to a preference for binding the smaller MeCN over PhCN. The opposite holds for **29b** since the cavity becomes larger upon removal of three *tert*-butyl groups. The rate of MeCN exchange is greatly enhanced for **29b** since there is no 'closing of the door' by the bulky substituents.

Polyimidazole binding sites of peptides can be mimicked by compounds **30**. The coordination geometry of their Cu^{2+} complexes is similar to that in **29** [57]. A water molecule located inside the cavity can selectively be exchanged by guest molecules like nitriles. In the absence of coordinated solvent molecules or a guest, di-, tri- and tetranuclear clusters are formed [58–60]. Cu^{+}-**30a** is able to bind CO inside its cavity. The C≡O stretch vibration in the resulting adduct is a very sensitive probe for changes in the supramolecular environment like in copper proteins [61]. Studies of complexes of **30a** with Co^{2+} and Ni^{2+} demonstrate the broad applicability of this spectroscopic technique in complexes incorporating metal ions other than Cu [62]. The water soluble Cu^{+}-**30b** is a stable Cu^{+} complex that does not undergo oxidation or dimerization [63].

The second generation ligand **31** (Fig. 20) contains an additional phenolic oxygen atom for metal binding [64]. This model for a tyrosine binding site can be oxidized into the corresponding phenoxyl radical and, therefore, play an important role in mimicking enzyme catalysis. Indeed, Cu^{+}-**31** undergoes fully reversible oxidation at low temperatures and is able to oxidize benzyl alcohol to benzaldehyde. The corresponding Zn^{2+}-bound tyrosinyl radical mimic is stable for hours and does not undergo reaction with benzyl alcohol.

The successful application of the third generation Cu^{2+}-**32** complex to enzyme mimicry by Izzet et al., is a clear highlight in this field of research [65]. This complex exhibits a remarkable stability and a very high affinity towards small neutral guests such as water, EtOH, DMF, and MeCN. The cuprous center undergoes defined and reversible redox chemistry. Thanks to the different affinities of Cu^{2+}/Cu^{+} for different guests, an electrochemically controlled ligand exchange could be performed: Cu^{2+}-bound DMF is expelled from the metal upon its oxidation and replaced by MeCN, which remains metal bound even after reduction. This may be considered as 'anti-thermodynamical' electro-driven ligand exchange.

Cu^{+}-**32** is able to activate molecular oxygen forming a Cu^{2+}-superoxide complex in a fast and irreversible way [66]. In a coordinating solvent like MeCN, the superoxide is released into the solution and substituted by a solvent molecule, whereas in the non-coordinating dichloromethane, the superoxide leads to oxygen insertion into the triethylene triamine (tren) ligand. On the basis of density functional theory (DFT) calculations using the B3LYP basis set the experimental IR data were attributed to the corresponding oxygen species bound to the metal ion thus gaining insight into mechanistic details of the superoxide decomposition [67,68].

The coordination of anionic guests was not possible with the third generation tren complex **32** (Fig. 20), whereas its pyridine analogue Cu^{+}-**33** (Fig. 21) is able to bind anions such as fluoride, azide, chloride, hydroxide, or alkoxide very efficiently [69]. This can be rationalized by steric differences between the complexes. In **32**, the phenolic oxygen atoms point towards the free coordination site of the metal and hamper the binding of anions by charge–dipole interactions. This is not the case in **33**, which consequently offers better access of the guest to the binding site. The redox chemistry of Cu^{+}-**33** is unique [70]. Whereas the acetonitrile complex of Cu^{+}-**33** does not react with molecular oxygen neither in solution nor in the solid state, the complex without enclosed acetonitrile undergoes defined oxidation in the solid state. The Cu^{+} center is able to activate one of the methylene bridges connecting the pyridine units to the calix[6]arene core. The resulting product contains a C=O group that inhibits further oxidation of the ligand. Calixarene **33** forms a Cu^{2+} complex with interesting redox behavior in cyclic voltammetry [71]. MeCN replaces DMF in Cu^{2+}-**33** (DMF) in dichloromethane only after reduction to Cu^{+} on the cyclic voltammetry timescale. This is attributed to the fact that the normally associative ligand exchange in Cu^{2+} species cannot take place in Cu^{2+}-**33** (DMF) due to the steric restriction by the rather small calix[6]arene funnel. Therefore, a fast dissociative exchange on the Cu^{+}-species occurs to yield Cu^{2+}-**33** (MeCN) after reoxidation. Thus, thermodynamically favored ligand exchanges can be suppressed by steric shielding of

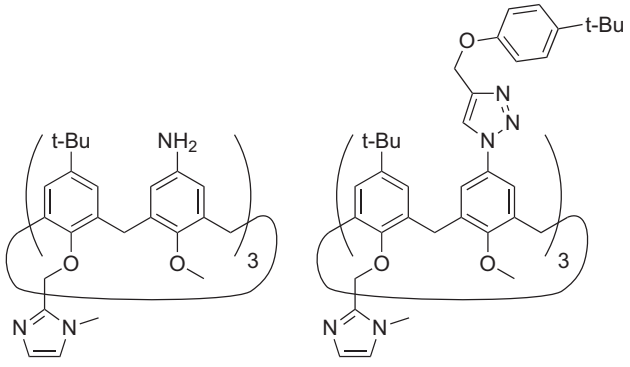

35 36

Fig. 22. Ditopic ligands of the first generation [78,81].

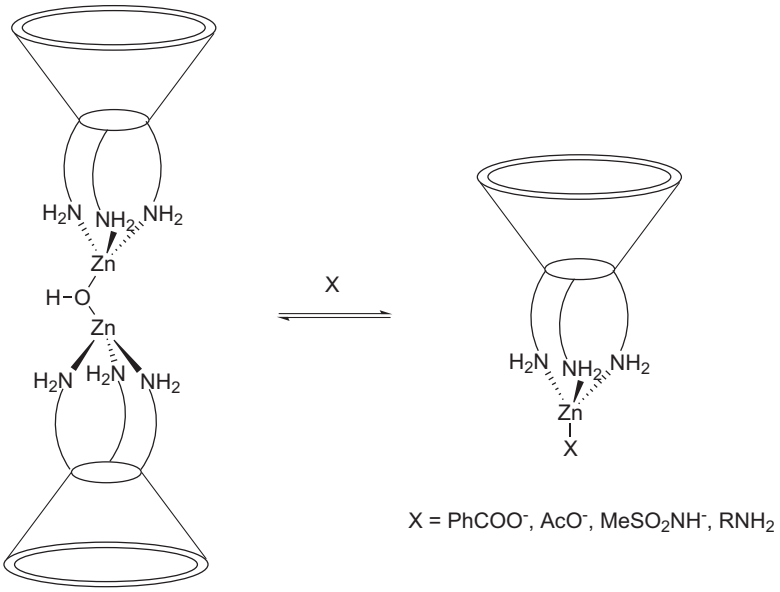

37

Fig. 23. Coordination driven disassembly of the dimeric complex **37** [83].

a weakly bound ligand. This gives evidence that only after preliminary reduction of the metal center in Cu^{2+} enzymes, coordination of a substrate may occur to initiate a catalytic cycle.

The replacement of the bridging *N*-atom in **33** by a phosphorous donor results in a very special complex **34** with a *P*-atom in axial *trans*-position with respect to the binding guest (Fig. 21) [72,73]. This leads to a higher selectivity for binding of the π-accepting DMF over MeCN or EtOH as compared to **33**.

3.2.2. Mononuclear Zn^{2+}-metalloprotein mimics

Pyrazole, benzimidazole, or methylimidazole attached to the calix[6]arene platform can form very stable, mononuclear complexes with tetrahedrally coordinated Zn^{2+} [74]. However, attached tertiary amines are too basic and lead to hydroxide precipitation, whereas pyridine forms very weak complexes [75]. The Zn^{2+} complex of **30a** (Fig. 19) exists as its aquo ion with the water molecule bound inside the cavity [76]. A second water molecule is held inside the cavity by hydrogen bonds with the metal bonded water molecule and a phenolic oxygen of the calixarene core and by OH/π stabilization. The two water molecules can be simultaneously replaced by amines, alcohols, nitriles or amides [74,77,78]. Sharp lines in ^{1}H NMR spectra for the encapsulated guest indicate that the exchange between free and encapsulated guest is slow on the NMR time scale.

Replacement of the three *tert*-butyl groups on the *upper rim* by primary amine functions to give the water soluble **35** (Fig. 22) opens the possibility for (a) coordination of a second Zn^{2+}-atom or (b) additional interactions with a host leading to better specificity [78–80].

When **35** is reacted with two Zn^{2+} atoms, a binuclear complex is formed that entraps an $(H_3O_2)^-$ ion as a bridging motif. In mononuclear Zn^{2+}-**35**, the imidazole units inside the cavity bind the metal ion. This complex is able to bind larger guests than its hexa-*tert*-butyl derivative **30a**, and in contrast to its binuclear analogue, complexes only a single water molecule. The aniline nitrogen atoms point towards the entrance of the cavity, thus blocking its access for other guests. Upon addition of a bulky guest, the cavity opens and the encapsulated water molecule is exchanged by for example benzylamine. This process goes along with a large change in the receptor's geometry (large induced fit), whereas small guests cause only a small change of the conformation. Hydrogen bonding between the aniline units in a MeCN complex leads to an increase of aniline basicity by about three pK_a units thus providing, in addition to the metal center and the hydrophobic cavity, a third recognition unit within the molecule.

The triazole containing **36** is able to bind a first Zn^{2+} ion inside the cavity through the imidazole units, whereas a second equivalent of metal ion can be bound to the triazoles [81]. Despite the limited accessibility of the cavity in the binuclear complex, the imidazole-bound Zn^{2+} can bind a nitrile anion. In contrast to Zn_2-**35**, where the free coordination sites of the metals point to each other, the second Zn^{2+} in Zn_2-**36** points outwards from the cavity and is able to bind a second guest on the periphery of the complex. A double displacement of two different metals was achieved in Cu/Zn^{2+}-**36** [82]. When Zn^{2+} is complexed at the *lower rim* imidazole units, the structure is rigidified such that the tetragonal Cu^{2+} cannot be complexed on the *upper rim* but Cu^+ is able to bind to the triazole units in this complex. If Cu^+/Zn^{2+}-**36** is oxidized to Cu^{2+}/Zn^{2+}-**36**, the metal ions swap places in the molecule. This observation might help to explain e.g. copper translocation within enzymes.

A bimetallic complex is obtained by coordination of the primary amino groups in calix[6]arene **37** (Fig. 23) with stoichiometric amounts of Zn^{2+} under formation of a μ-hydroxo-bridge [83]. Coordination of a guest outside the cavity is possible because the primary amines are sterically not demanding and thus allow coordination of the metal outside of the basket. The hydroxo-dimer can be converted into monomeric complexes using e.g. carboxylic acids, sulfonamides or primary amines. Guest binding studies of the different dimer/monomers revealed that the selectivity for guests can be efficiently controlled by the charge of the resulting complex. The second generation ligand **31b** forms three different monomeric Zn^{2+} complexes [84]. A dicationic complex is formed by complexation of the metal ion by the two imidazole units and the phenolic hydroxide. The latter can be deprotonated to yield a monocationic phenolate complex. The third species can be obtained by addition of hydroxide or chloride that coordinates to the metal center from the outside of the cavity. In this neutral compound the normally 5-coordinate metal center undergoes a change of coordination number from five to four by release of an imidazole

pendant arm. The affinity for guests decreases in the order dicationic > monocationic > neutral.

The third generation Zn-**32** is stabilized by a coordinating MeCN molecule and does not undergo dimerization [85]. This ternary compound is stable against anion coordination under basic conditions due to the strong chelate effect of the tren unit.

All calixarene based metalloenzyme mimics described here are so much reduced in complexity compared to the natural parent systems that they do not allow to study all of the enzymes' features with one model complex. Rather, they shed some light on specific features of enzymes and the way they function. Whereas most calix[4]arene based systems are catalytically active, they cannot compete with natural systems in terms of activity, selectivity and substrate diversity but they can help to understand which effects variations in metal–metal distances in multinuclear metalloenzymes can have, how important a certain degree of flexibility of the enzyme's active site is for efficient substrate binding and how subtle changes can block or boost catalytic activity. The calix[6]arene based enzyme mimics studied up to now do not possess catalytic activity. The rationale for their use as enzyme mimics is that they allow one to study the (redox) chemistry of the central metal ions, give clues of how guest binding can be controlled by the design of the pocket and show conformational changes around the active sites occurring upon substrate binding. Furthermore, some new evidence has been gained that can explain how metal exchanges or translocations might occur in a controlled way in metalloenzymes. The very elegant chemistry of these calix[6]arene based mimics could not yet contribute much to the understanding of natural metalloenzymes but the observations so far clearly indicate that more sophisticated systems will be able to shed light on mechanistic aspects of metalloenzymes.

3.2.3. *Metalloenzyme inhibitors*

As described above, some phosphatases have two Zn^{2+} ions in their active site. Compounds that have high affinities to the metal centers and block the access of the substrate can efficiently inhibit these enzymes (Fig. 24).

Calixarenes **38** and **39** are, for example, good inhibitors for calf intestine alkaline phosphatase (Fig. 25) [86,87]. The methylenebisphosphonates are able to interact with the enzyme's active site by complex formation. The hydrophobic calix[4]arene could provide additional interactions with the pocket of the enzyme. Amino functionalization of the phosphonate pendant arms leads to chiral isomers that show different inhibition activity depending on the absolute stereochemistry.

Interestingly, tests on *Yersinia* bacteria that have one of the most active protein tyrosine phosphatases (PTP's) with various calixarenes (amongst which **38–40**) showed that especially **40** can

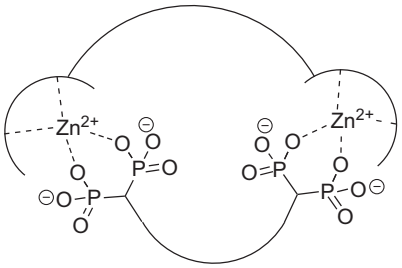

Fig. 24. Proposed mechanism of the inhibition of Zn-containing phosphatases by bisphosphonates.

inhibit the PTP (K_A = 0.92 μM), which is an outer membrane protein of the bacterium [88]. PTP's catalyze the dephosphorylation of phosphotyrosine residues in proteins but do not have a metal center in their active side. Nevertheless, interactions with metal ions and the phosphonato-calixarenes and a resulting effect on the bacteria cannot be excluded. *Yersinia* bacteria can cause diseases ranging from gastrointestinal syndromes to bubonic plague. The inhibition of PTP's of these bacteria could open the way for new therapeutics for diseases caused by *Yersinia* bacteria but this has yet to be tested in clinical trials.

4. Agents for radiotherapy and medical imaging

As already mentioned before, calix[4]arene derivatives are able to form stable complexes with main group and transition metal ions. For some medical purposes, lanthanides or actinides are of great interest. Already in the early days of calixarene chemistry, it was found that calixarenes can bind those trivalent cations very efficiently [89].

4.1. *Radiotherapy*

Ionizing radiation can be used effectively in the treatment of cancer. To minimize the damage of healthy cells, radioactive metal ions are complexed by strong chelators, which are coupled to e.g. antibodies or specific peptides to deliver the agent to the diseased site and thus avoiding the damage of healthy tissue. Crucial for successful application of such systems are bifunctional ligands that can be attached to a targeting vector and form very stable complexes with radionuclides. An attractive isotope for radiotherapy is the α-emitter $^{225}Ac^{3+}$ which has a half-life time of 10 days. Calixarenes of type **41** were prepared and their Ac^{3+} coordination was studied (Fig. 26). The binding to receptors and immune response of mice of these complexes were reported [90].

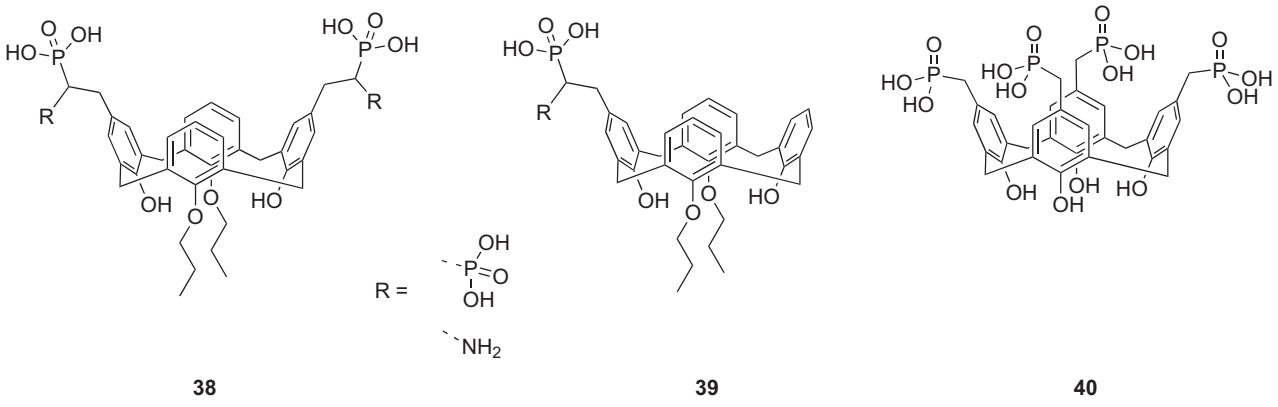

Fig. 25. Alkaline phosphatase and protein tyrosine phosphatase inhibitors [86–88].

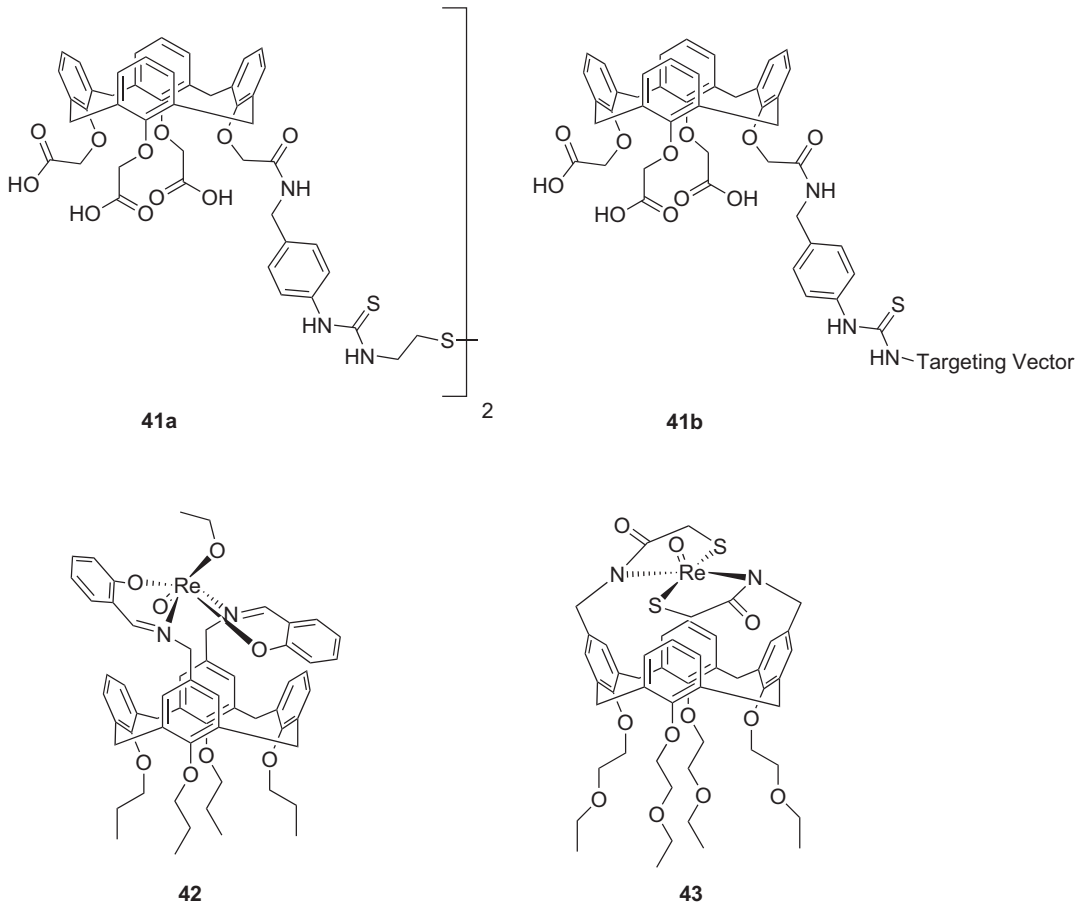

Fig. 26. Calixarenes for radiotherapy [90,92].

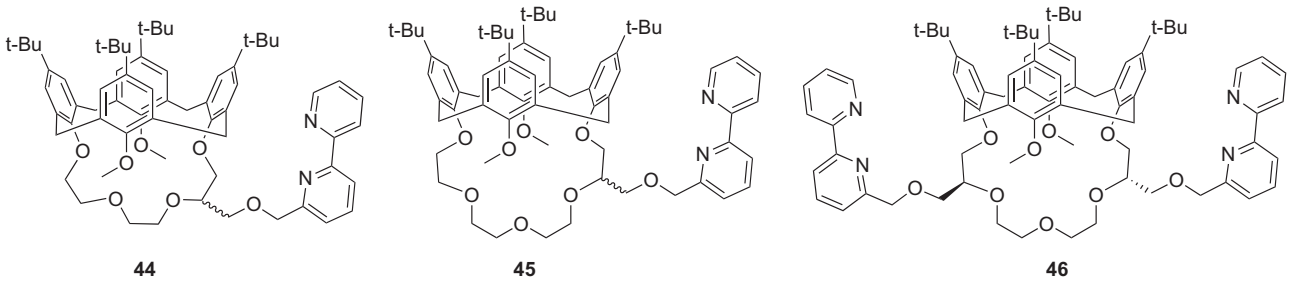

Fig. 27. Lanthanide chelators for luminescence studies[93].

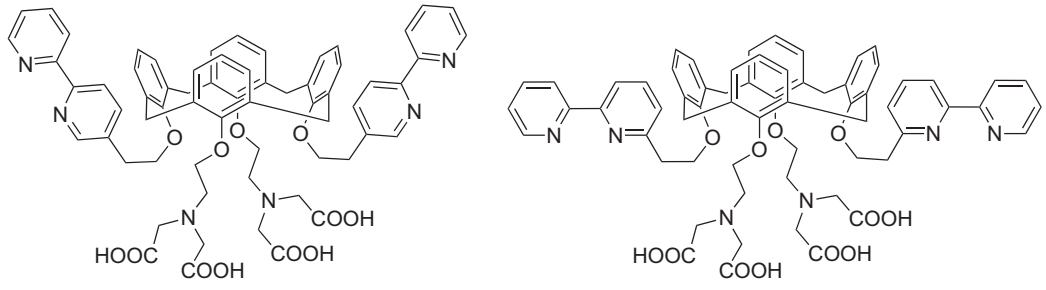

Fig. 28. Strong chelators for luminescent lanthanide ions [94].

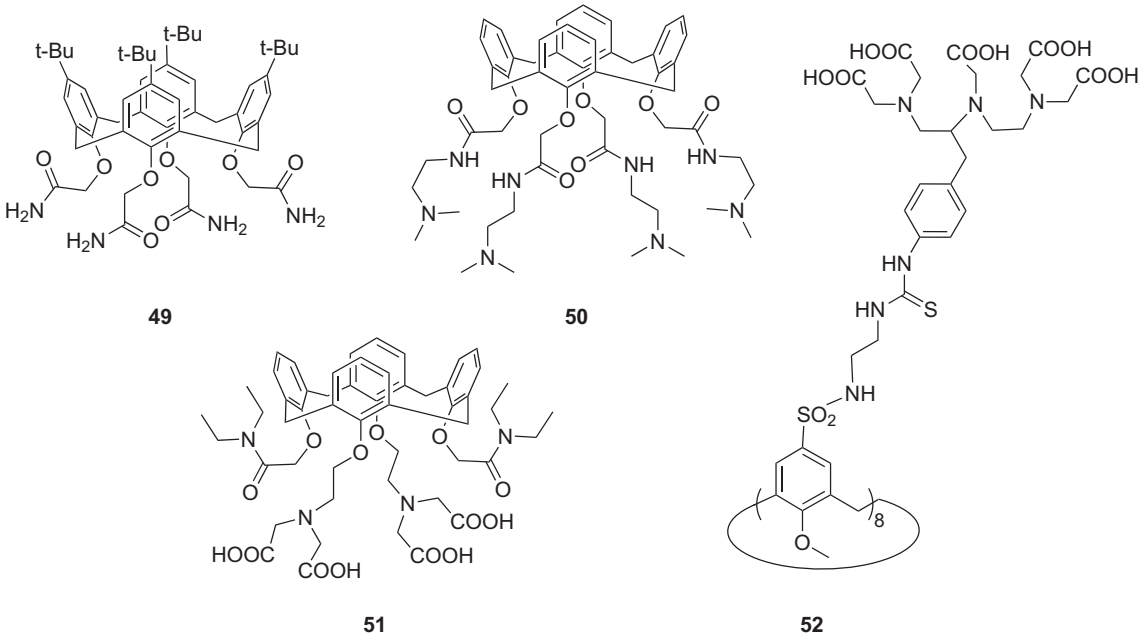

Fig. 29. Calixarene based chelators for MRI contrast agents [96,97].

In vivo tests of **41a/b** in mice showed that the binding to the target strongly depends on the nature of the targeting vector (antibodies or peptides), the dosage and the injection method. The authors conclude that the conjugation of **41b** to humanized antibodies will probably not lead to an immune response, while the targeting will not be disturbed. It may be doubted whether the complexation of Ac^{3+} by the carboxylates and the amide carbonyl of **41** is strong enough to prevent leaching of the metal ion under physiological conditions (Fig. 26).

Complexation studies of ^{230}U with the sulfo-calix[6 and 8]arene analogues of **28b** performed in blood serum show that although the complexation of uranium by such ligands is efficient, serum proteins and carbonate lead to the destruction of the desired complexes [91]. Therefore, *in vivo* application of such compounds is not possible.

The most prominent transition metals used for radiotherapy are ^{99m}Tc and the β^--emitting ^{186}Re and ^{188}Re. Re(V) can be efficiently complexed by for example N_2O_2- or N_2S_2-donors that are prearranged properly. Therefore, **42** and **43** were prepared [92]. Unfortunately, apart from the information that **43** is stable in PBS, no further characterization relevant for possible applications was performed.

4.2. Luminescent agents

The lanthanides Eu^{3+} and Tb^{3+} are widely used as luminescent probes. Because of their toxicity, they need to be complexed by strong chelators. The complexation is also necessary to shield the metal ions from coordination of water, which would quench the luminescence. To enhance their luminescent properties, organic antenna molecules that bind to the metal ions are used for effective sensitization. The advantage of lanthanide based probes compared to organic agents is that the emission bands are extremely narrow and therefore, those agents are more sensitive than organic dyes.

Both the Eu^{3+} and Tb^{3+} complexes of the bipyridyl containing **44–46** (Fig. 27) have very promising luminescence properties in acetonitrile, but their solubility in water is not sufficient [93]. When a water molecule is bound to a luminescent ion, it quenches its luminescence rather efficiently. Therefore, studies need to be performed in water to know whether these systems are suitable for bioimaging. Attachment of two bipyridyl groups to a di-iminodiacetic acid calix[4]arene backbone resulted in chelators **47** and **48** (Fig. 28) that form very stable, strongly luminescent complexes especially with Tb^{3+} [94]. These compounds are still not sufficiently water soluble but the results of luminescence studies performed in methanol, that has a quenching effect similar to water, are very promising. These studies also showed that the quantum yield is independent on whether the bipyridyl units are attached to the calixarene via their 3- or 4-position.

4.3. Magnetic resonance imaging (MRI) contrast agents

In most clinical magnetic resonance imaging (MRI) scans, the ^1H signal of water protons is observed and the image reflects either the proton density or differences in the longitudinal (T_1) or transversal (T_2) relaxation time of water protons in certain compartments of the body. The majority of MRI contrast agents contain Gd^{3+}-ions that are able to shorten the T_1 relaxation times of surrounding water molecules very efficiently and lead to a brightening in MR images of areas that contain the agent [95]. The ability of an agent to shorten T_1 is expressed as longitudinal proton relaxivity (r_1), which is the relaxation rate enhancement of water protons in $s^{-1}mM^{-1}$ Gd^{3+}. Because the dose of an MRI contrast agent required to obtain good contrast is much higher than for luminescence probes, the thermodynamic and kinetic inertness of the complexes is of utmost importance to prevent adverse side effects to the patient. Therefore, there is a need to develop chelators that are able to bind Gd^{3+} very efficiently and have high relaxivity.

In a first study towards calixarene based MRI contrast agents, calix[4]arene tetraamide **49** (Fig. 29) was used to chelate Gd^{3+} [96]. The relaxivity of this complex in a dmso/water mix (9:1) at 20 °C and 400 MHz is 3.40 s^{-1} mM^{-1}, the stability constant is about 1000 M^{-1}. For practical applications, the stability and the water solubility are much too low and, therefore, no further studies on this compound were performed.

A more stable Gd-complex is formed with **50** [97]. The presence of four additional chelating groups results in the formation of an octa-coordinated metal ion and an increase of the stability constant to 2×10^5 M^{-1}, which is still too low for practical applica-

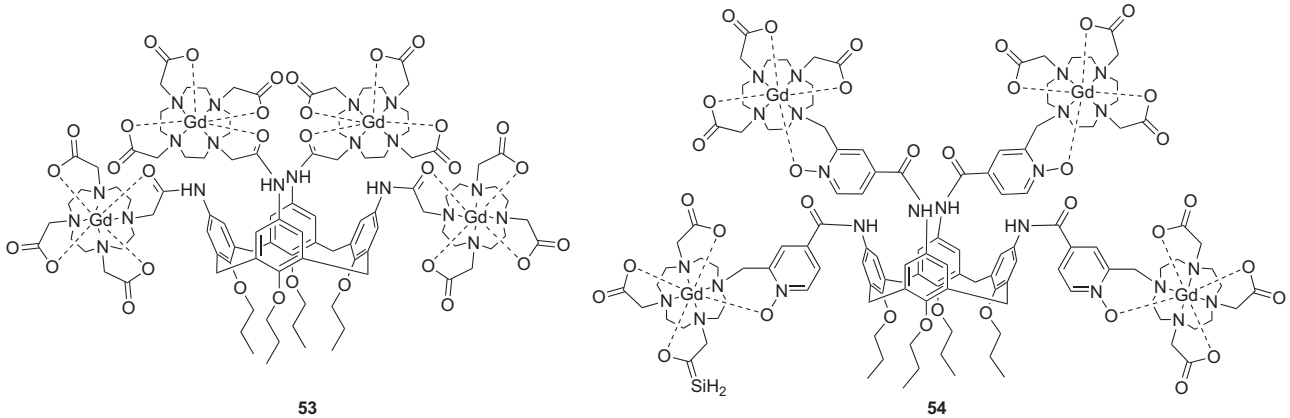

Fig. 30. Self-aggregating MRI contrast agents [100,101].

tions. This compound interacts with human serum albumin (HSA) and, therefore, opens the way to the development of new, water soluble calixarene based MR angiography agents.

Casnati and co-workers used di-imidodiacetic acid functionalized calixarene **51** for Gd^{3+} complexation and found a stability constant of greater than $10^{13}\,M^{-1}$ [98]. The relaxivity of the free complex is $9.6\,s^{-1}\,mM^{-1}$ at 20 MHz and 25 °C. The HSA-adduct is rather stable ($K_A = 2.4 \times 10^4\,M^{-1}$) and has a relaxivity of as high as $60\,s^{-1}\,mM^{-1}$. Interestingly, the unbound compound has three inner-sphere water molecules ($q = 3$), whereas its HSA-adduct has only one. This can be explained by the fact that in the free form, the amide groups do not participate in the metal binding whereas in the complex with albumin, for example aspartate or glutamate binds to the metal and thus, increases the stability of the resulting adduct.

Compound **52** can form a stable complex with eight Gd^{3+} ions, with a stepwise formation constant for each Gd^{3+} ion of more than $10^{17}\,M^{-1}$ [99]. This compound is also highly soluble in water, which makes it the first calixarene based MRI contrast agent reported that could be used for *in vivo* studies. Unfortunately, no parameters describing the suitability of this compound as a contrast agent in terms of relaxivity were given.

The attachment of cyclic 1,4,7,10-tetra(carboxymethyl)-1,4,7,10-tetraazacyclododecane (DOTA) based chelators to the calixarene core leads to efficient contrast agents. Compound **53** (Fig. 30) is a highly rigid compound both as monomer and in micellar aggregates [100]. It forms spherical micelles above a critical micelle concentration (cmc) of 0.21 mM at 37 °C with a hydrodynamic radius of 2.2 nm. The high rigidity leads to relaxivities up to $18.3\,s^{-1}\,mM^{-1}$ at 20 MHz and 37 °C. Upon HSA binding, this compound ($K_A = 1.2 \times 10^3\,M^{-1}$) has good relaxivities ($24.6\,s^{-1}\,mM^{-1}$ at 20 MHz and 37 °C). The relaxivity-limiting factor of this system is a relatively slow exchange rate k_{ex} between water molecules bound to the Gd-centers and bulk water. Calixarene **54** contains four pyridine-*N*-oxide chelating units that are known to have close to optimal water exchange kinetics [101]. This compound has remarkable relaxivities of $31.2\,s^{-1}\,mM^{-1}$ at 20 MHz and 25 °C in form of its micelles (radius 8.2 nm, cmc = 35 μM, see Fig. 30). Binding of the monomer to HSA leads to solutions with observed relaxivities of up to $40.8\,s^{-1}\,mM^{-1}$ at 20 MHz and 37 °C in the presence of 2.0 mM albumin. This compound has a density of relaxivity of $39.2\,g\,l^{-1}\,s^{-1}$, which is one of the highest values reported so far. The density of relaxivity is a measure of the relaxivity per mass unit contrast agent and is of great importance for practical applications in MRI.

The inclusion of bis-octadecyl calixarene derivative, **55**, into the membrane of DSPC-based liposomes yielded nano-containers with very good relaxivities (Fig. 31) [102]. This was attributed to the fact

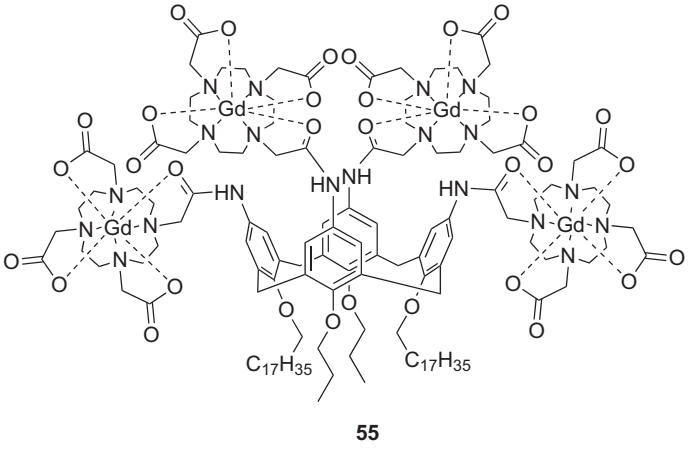

Fig. 31. Calixarene **55** for inclusion in the outer surface of liposomal membranes [102].

that a majority (at least 80%) of **55** is oriented on the outer surface of the liposomes. In general, Gd-atoms that are entrapped inside liposomes have a low contribution to the relaxivity due to the limited propagation of their effect to the bulk water due to the slow diffusion of water molecules across the membrane. Aggregates of **55** have a large potential in multimodal imaging since e.g. radioactive material can be included in their interior (for PET and SPECT imaging) or fluorescent dyes can be included in either the membrane or the cavity of the liposomes.

5. Other applications

Carboxylic acid based di- and tetranuclear Sn(IV) complexes and their anticancer and antibacterial activity are well documented in the literature [103]. In a recent paper, the beneficial effect of such compounds **56** (Fig. 32) on the suppression of blood and tissue oxidative stress caused by lead in male albino Wistar rats was investigated [104]. The positive effect was attributed to the binding of **56** to cysteine moieties in peptides, which then hampers the binding of lead.

Cell cycle progression is dependent on the intracellular iron level since iron-containing proteins catalyze key reactions involved in e.g. DNA synthesis. In particular, ribonucleotide reductase activity is dependent on the intracellular iron level. Since this activity is crucial in the rate-limiting step in DNA synthesis, there is potential to target iron with chemotherapeutics [105]. Attempts to use calix[4]arene based iron chelators to decrease cell viability on the human hepatocarcinoma HepaRG cell line showed that the tested

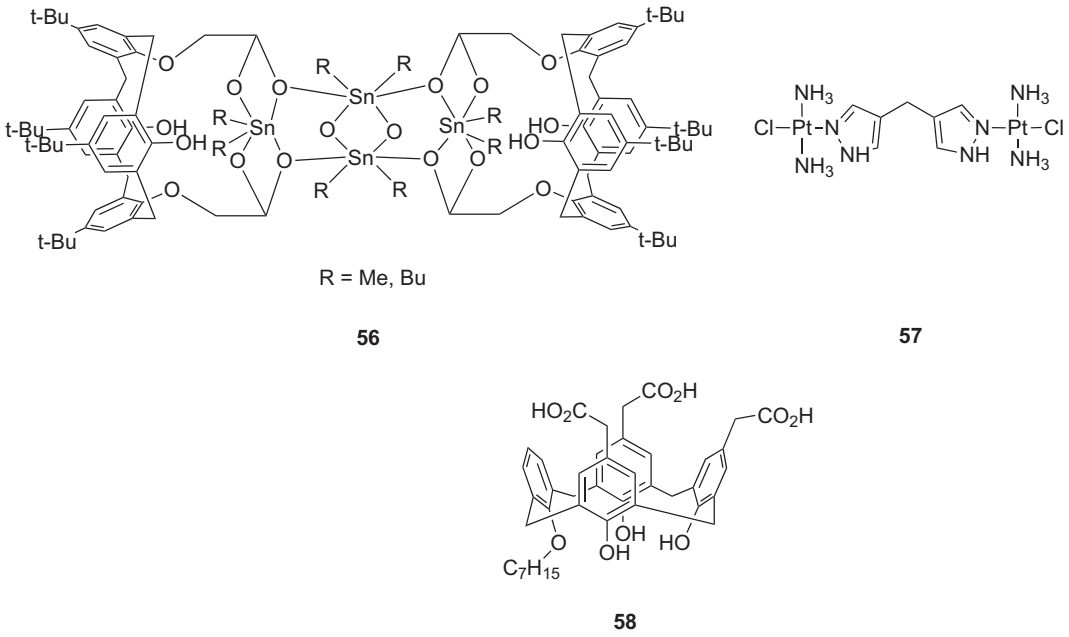

Fig. 32. Structures of a Sn(IV) based anti-lead agent and of a cisplatin derivative [104,109,110].

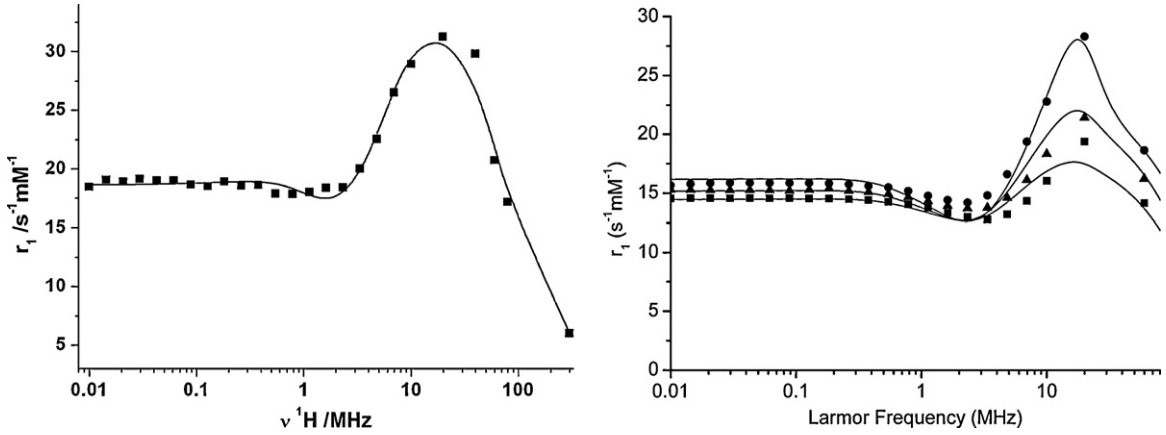

Fig. 33. Nuclear magnetic relaxation dispersion (NMRD) profiles of left: a 925 μM solution of micellar **54** at 25 °C and right: a liposomal suspension of **55** included in DSPC-based liposomes (8.8 mol% of total formulation) at 25 °C (squares), 37 °C (triangles) and 55 °C (circles). The curves indicate the result from the fitting to a theoretical model [101,102].

calixarenes do not bind iron but can decrease cell viability due to other effects on their cytotoxicity [106,107].

One of the most prominent chemotherapeutics is cisplatin [108]. Compared to cisplatin, **57** is less cytotoxic in human ovarian cancer cell lines (Fig. 33). Sulfonatocalix[4]arene **28b** was tested as a drug delivery agent for **57** and for a possible activity enhancement [109]. The platinum complex interacts with the calixarene via ionic interactions as well as hydrogen bonding between its amino groups and the sulfonato moieties of **28b**, whereas, the hydrophobic dipyrazolylmethane part is complexed by the calixarene cavity. However, no change in activity of **57** in the presence of **28b** was observed which is due the low stability of the complex *in vitro*.

Tricarboxycalixarene **58** exhibits a high affinity towards the NBD1 domain of the MRP1 protein. Using fluorescence spectroscopy it has been proven that this binding process is dependent on the availability of magnesium ions. The association is of the same order as that observed for the natural substrate ATP-Mg [110].

Cutaneous contamination represents the second highest contamination pathway in the nuclear industry. An oil-in-water nano-emulsion containing the calix[6]arene shown in Fig. 18 (R = CH_2COOH) was investigated in terms of its suitability to remove uranium from skin. Thanks to the high binding affinity of this calixarene to uranyl, the transcutaneous uranyl uptake through skin was decreased by 98% [111].

6. Conclusion

In summary, calixarenes are multifunctional building blocks for many (biological) applications. They show very good properties as artificial ion channels, metalloenzyme mimics/inhibitors and can be used in radiotherapy and medical imaging. In many applications, calixarenes are only used as synthetic platforms to prearrange functional groups in a three-dimensional space. The ion transport through artificial cell membranes (partial dehydration of the ion) directly benefits from the presence of the hydrophobic basket. In some cases, this is also beneficial for the substrate binding in enzyme mimics. Even though calixarene based ion channels are already quite sophisticated, there are still many challenges to be addressed by the enzyme mimics. In the case of calix[4]arene based

mimics, the catalytic properties of the complexes are good but there are only a few cases where the calixarene is more than a spacer between functional groups. Calix[6]arenes are the more promising mimics since they show a direct use of the calixarene itself with surprising similarities to natural systems. To achieve real catalysis with these systems is a challenge that remains to be tackled. In radiotherapy and medical imaging, calixarenes can be used as synthetic platforms that allow the attachment of metal chelates. The hydrophobic nature of the calixarene backbone may lead to hepatic uptake. If this is not desired, it can be circumvented by attaching hydrophilic moieties to the agents or by including them in e.g. liposomes. Benefits for applications in these fields are that calixarenes are able to carry a high payload of metal ions and thus, to multiply the desired properties of mononuclear analogues.

Acknowledgment

D.T.S. thanks the EU for a Marie-Curie training site host fellowship (MEST-CT-2004-7442). This work was performed in the frame of COST D38 (Metal-Based Systems for Molecular Imaging Applications) and the European Network of Excellence EMIL (European Molecular Imaging Laboratories) program LSCH-2004-503569.

References

[1] L. Mandolini, R. Ungaro, Calixarenes in Action, Imperial College Press, London, 2000.
[2] J. Vicens, V. Böhmer, Calixarenes, a Versatile Class of Macrocyclic Compounds, Kluwer, Dordrecht, 1991.
[3] R.V. Rodik, V.I. Boyko, V.I. Kalchenko, Curr. Med. Chem. 16 (2009) 1630–1655.
[4] B.S. Creaven, D.F. Donlon, J. McGinley, Coord. Chem. Rev. 253 (2009) 893–962.
[5] Y.K. Agrarwal, H. Bhatt, Bioinorg. Chem. Appl. 2 (2004) 237–274.
[6] O. Danylyuk, K. Suwinska, Chem. Commun. (2009) 5799–5813.
[7] A. Dondoni, A. Marra, Chem. Rev. 110 (2010) 4949–4977.
[8] C.D. Gutsche, Calixarenes, RSC, Cambridge, 1989.
[9] C.D. Gutsche, Calixarenes Revisited, RSC, Cambridge, 1998.
[10] Z. Asfari, V. Böhmer, H. Harrowfield, J. Vicens, Calixarenes 2001, Kluwer, Dordrecht, 2001.
[11] C.D. Gutsche, Calixarenes: An Introduction, RSC, Cambridge, 2008.
[12] J. Vicens, J. Harrowfield, L. Baklouti, Calixarenes in the Nanoworld, Springer, Dordrecht, 2007.
[13] L. Baldini, A. Casnati, F. Sansone, R. Ungaro, Chem. Soc. Rev. 36 (2007) 254–266.
[14] F. Perret, A.N. Lazar, A.W. Coleman, Chem. Commun. (2006) 2425–2438.
[15] K.S.J. Iqbal, P.J. Cragg, Dalton Trans. (2007) 26–32.
[16] J.W. Cornforth, P.D. Hart, G.A. Nicholls, R.J. Rees, J.A. Stock, Br. J. Pharmacol. 10 (1955) 73–86.
[17] M.J. Colston, H.C. Hailes, E. Stavropoulos, A.C. Hervé, G. Hervé, K.J. Doodworth, A.M. Hill, P. Jenner, P.D. Hart, R.E. Tacson, Infect. Immun. 72 (2004) 6318–6323.
[18] L. Mutihac, Curr. Drug Discov. Technol. 5 (2008) 98–104.
[19] L. Mutihac, Anal. Lett. 43 (2010) 1355–1366.
[20] T. Jin, Chem. Commun. (2000) 1379–1380.
[21] M.A. Klyachina, V.I. Boyko, A.V. Yakovenko, L.G. Babich, S.G. Shlykov, S.O. Kosterin, V.P. Khilya, V.I. Kalchenko, J. Incl. Phenom. Macrocycl. Chem. 60 (2008) 131–137.
[22] R. Rodik, V. Boiko, O. Danylyuk, K. Suwinska, I. Tsymbal, N. Slinchenko, L. Babich, S. Shlykov, S. Kosterin, J. Lipkowski, V. Kalchenko, Tetrahedron Lett. 46 (2005) 7459–7462.
[23] T. Jin, M. Kinjo, Y. Kobayashi, H. Hirata, Faraday Trans. 94 (1998) 3135–3140.
[24] N. Maulucci, F.D. Riccardis, C.B. Botta, A. Casapullo, E. Cressina, M. Fregonese, P. Tecilla, I. Izzo, Chem. Commun. (2005) 1354–1356.
[25] K.S.J. Iqbal, M.C. Allen, F. Fucassi, P.J. Cragg, Chem. Commun. (2007) 3951–3953.
[26] J.C. Iglesias-Sánchez, W. Wang, R. Ferdani, P. Prados, J. de Mendoza, G.W. Gokel, New J. Chem. 32 (2008) 878–890.
[27] D.T. Schühle, S. Klimosch, J. Schatz, Tetrahedron Lett. 49 (2008) 5800–5803.
[28] A. Arduini, A. Credi, G. Faimani, C. Massera, A. Pochini, A. Secchi, M. Semeraro, S. Silvi, F. Ugozzoli, Chem. Eur. J. 14 (2008) 98–106.
[29] J.C. Mareque Rivas, H. Schwalbe, S.J. Lippard, Proc. Natl. Acad. Sci. 98 (2001) 9478–9483.
[30] S.E. Matthews, P. Schmitt, V. Felix, M.G.B. Drew, P. de Beer, J. Am. Chem. Soc. 124 (2002) 1341–1353.
[31] M.J. Wiester, P.A. Ulmann, C.A. Mirkin, Angew. Chem. Int. Ed. 50 (2011) 114–137.
[32] D.M. Homden, C. Redshaw, Chem. Rev. 108 (2008) 5086–5130.
[33] P. Molenveld, J.F.J. Engbersen, D.N. Reinhoudt, Eur. J. Org. Chem. 12 (1999) 3269–3275.
[34] P. Molenveld, J.F.J. Engbersen, D.N. Reinhoudt, Chem. Soc. Rev. 29 (2000) 75–86.
[35] P. Molenveld, W.M.G. Stikvoort, H. Kooijman, A.L. Spek, J.F.J. Engbersen, D.N. Reinhoudt, J. Org. Chem. 64 (1999) 3896–3906.
[36] R. Cacciapaglia, A. Casnati, L. Mandolini, D.N. Reinhoudt, R. Salvio, A. Sartori, R. Ungaro, J. Org. Chem. 70 (2005) 624–630.
[37] P. Molenveld, J.F.J. Engbersen, D.N. Reinhoudt, Angew. Chem. Int. Ed. 38 (1999) 3189–3192.
[38] R. Cacciapaglia, A. Casnati, L. Mandolini, D.N. Reinhoudt, R. Salvio, A. Sartori, R. Ungaro, J. Org. Chem. 70 (2005) 5398–5402.
[39] D.J.E. Spencer, B.J. Johnson, W.B. Tolman, Org. Lett. 4 (2002) 1391–1393.
[40] R. Cacciapaglia, A. Casnati, L. Mandolini, D.N. Reinhoudt, R. Salvio, A. Sartori, R. Ungaro, J. Am. Chem. Soc. 128 (2006) 12322–12330.
[41] R. Cacciapaglia, A. Casnati, L. Mandolini, D.N. Reinhoudt, R. Salvio, A. Sartori, R. Ungaro, Inorg. Chim. Acta 360 (2007) 981–986.
[42] G. Ozturk, E.U. Akkaya, Org. Lett. 6 (2004) 241–243.
[43] R. Cacciapaglia, A. Casnati, L. Mandolini, A. Peracchi, D.N. Reinhoudt, R. Salvio, A. Sartori, R. Ungaro, J. Am. Chem. Soc. 129 (2007) 12512–12520.
[44] P. Molenveld, J.F.J. Engbersen, D.N. Reinhoudt, J. Org. Chem. 64 (1999) 6337–6341.
[45] Y. Cao, Q. Zheng, C. Chen, H. Hu, Z. Huang, Inorg. Chim. Acta 357 (2004) 316–320.
[46] L. Baldini, C. Bracchini, R. Cacciapaglia, A. Casnati, L. Mandolini, R. Ungaro, Chem. Eur. J. 6 (2000) 1322–1330.
[47] R. Cacciapaglia, A. Casnati, S.D. Stefano, L. Mandolini, D. Paolemili, D.N. Reinhoudt, A. Sartori, R. Ungaro, Chem. Eur. J. 10 (2004) 4436–4442.
[48] J.L. Atwood, G.W. Orr, N. Carlene Means, F. Hamada, H. Zhang, S.G. Bott, K.D. Robinson, Inorg. Chem. 31 (1992) 603–606.
[49] R. Fiammengo, K. Wojciechowski, M. Crego-Calama, P. Timmerman, A. Figoli, M. Wessling, D.N. Reinhoudt, Org. Lett. 5 (2003) 3367–3370.
[50] H. Bakirci, A.L. Koner, M.H. Dickman, U. Kortz, W.M. Nau, Angew. Chem. Int. Ed. 45 (2006) 7400–7404.
[51] S. Blanchard, L.L. Clainche, M. Rager, B. Chansou, J. Tuchagues, A.F. Duprat, Y.L. Mest, O. Reinaud, Angew. Chem. Int. Ed. 37 (1998) 2732–2735.
[52] N. Le Poul, M. Campion, B. Douziech, Y. Rondelez, L. Le Clainche, O. Reinaud, Y. Le Mest, J. Am. Chem. Soc. 129 (2007) 8801–8810.
[53] N. Le Poul, M. Campion, G. Izzet, B. Douziech, O. Reinaud, Y. Le Mest, J. Am. Chem. Soc. 127 (2005) 5280–15280.
[54] S. Blanchard, M. Rager, A.F. Duprat, O. Reinaud, New J. Chem. 22 (1998) 1143–1146.
[55] Y. Rondelez, M. Rager, A. Duprat, O. Reinaud, J. Am. Chem. Soc. 124 (2002) 1334–1340.
[56] L. Le Clainche, M. Giorgi, O. Reinaud, Inorg. Chem. 39 (2000) 3436–3437.
[57] G. Izzet, Y.M. Frapart, T. Prangé, K. Provost, A. Michalowicz, O. Reinaud, Inorg. Chem. 44 (2005) 9743–9751.
[58] G. Izzet, H. Akdas, N. Hucher, M. Giorgi, T. Prangé, O. Reinaud, Inorg. Chem. 45 (2006) 1069–1077.
[59] O. Sénèque, M. Campion, B. Douziech, M. Giorgi, E. Rivière, Y. Journaux, Y. Le Mest, O. Reinaud, Eur. J. Inorg. Chem. 8 (2002) 2007–2014.
[60] Y. Rondelez, O. Sénèque, M. Rager, A. Duprat, O. Reinaud, Chem. Eur. J. 6 (2000) 4218–4226.
[61] O. Sénèque, M. Campion, M. Giorgi, Y. Le Mest, O. Reinaud, Eur. J. Inorg. Chem. 9 (2004) 1817–1826.
[62] Y. Rondelez, G. Bertho, O. Reinaud, Angew. Chem. Int. Ed. 41 (2002) 1044–1046.
[63] O. Sénèque, M. Campion, B. Douziech, M. Giorgi, Y.L. Mest, O. Reinaud, Dalton Trans. (2003) 4216–4218.
[64] G. Izzet, B. Douziech, T. Prangé, A. Tomas, I. Jabin, Y. Le Mest, O. Reinaud, Proc. Natl. Acad. Sci. 102 (2005) 6831–6836.
[65] G. Izzet, J. Zeitouny, H. Akdas-Killig, Y. Frapart, S. Ménage, B. Douziech, I. Jabin, Y. Le Mest, O. Reinaud, J. Am. Chem. Soc. 130 (2008) 9514–9523.
[66] A. De la Lande, H. Gérard, V. Moliner, G. Izzet, O. Reinaud, O. Parisel, J. Biol. Inorg. Chem. 11 (2006) 593–608.
[67] A. De la Lande, O. Parisel, H. Gérard, V. Moliner, O. Reinaud, Chem. Eur. J. 14 (2008) 6465–6473.
[68] G. Izzet, X. Zeng, H. Akdas, J. Marrot, O. Reinaud, Chem. Commun. (2007) 810–812.
[69] G. Izzet, X. Zeng, D. Over, B. Douziech, J. Zeitouny, M. Giorgi, I. Jabin, Y. Le Mest, O. Reinaud, Inorg. Chem. 46 (2007) 375–377.
[70] G. Thiabaud, G. Guillemot, I. Schmitz-Afonso, B. Colasson, O. Reinaud, Angew. Chem. Int. Ed. 48 (2009) 7383–7386.
[71] N. Le Paul, B. Douziech, J. Zeitouny, G. Thiabaud, H. Colas, F. Conan, N. Cosquer, I. Jabin, C. Lagrost, P. Hapiot, O. Reinaud, Y. Le Mest, J. Am. Chem. Soc. 131 (2009) 17800–17807.
[72] D. Over, A. de la Lande, X. Zeng, O. Parisel, O. Reinaud, Inorg. Chem. 48 (2009) 4317–4330.
[73] O. Sénèque, M. Rager, M. Giorgi, O. Reinaud, J. Am. Chem. Soc. 122 (2000) 6183–6189.
[74] O. Sénèque, Y. Rondelez, L. Le Clainche, C. Inisan, M. Rager, M. Giorgi, O. Reinaud, Eur. J. Inorg. Chem. 10 (2001) 2597–2604.
[75] O. Sénèque, M. Rager, M. Giorgi, O. Reinaud, J. Am. Chem. Soc. 123 (2001) 8442–8443.
[76] O. Sénèque, M. Giorgi, O. Reinaud, Supramol. Chem. 15 (2003) 573–580.
[77] O. Sénèque, M. Giorgi, O. Reinaud, Chem. Commun. (2001) 984–985.
[78] D. Coquière, J. Marrot, O. Reinaud, Chem. Commun. (2006) 3924–3926.
[79] D. Coquière, J. Marrot, O. Reinaud, Org. Biomol. Chem. 6 (2008) 3930–3934.
[80] D. Coquière, A. de la Lande, S. Marti, O. Parisel, T. Prangé, O. Reinaud, Proc. Natl. Acad. Sci. 106 (2009) 10449–10454.

[81] B. Colasson, M. Save, P. Milko, J. Roithová, D. Schröder, O. Reinaud, Org. Lett. 9 (2007) 4987–4990.
[82] B. Colasson, N. Le Paul, Y. Le Mest, O. Reinaud, J. Am. Chem. Soc. 132 (2010) 4393–4398.
[83] U. Darbost, O. Sénèque, Y. Li, G. Bertho, J. Marrot, M. Rager, O. Reinaud, I. Jabin, Chem. Eur. J. 13 (2007) 2078–2088.
[84] O. Sénèque, M. Rager, M. Giorgi, T. Prangé, A. Tomas, O. Reinaud, J. Am. Chem. Soc. 127 (2005) 14833–14840.
[85] U. Darbost, X. Zeng, M. Rager, M. Giorgi, I. Jabin, O. Reinaud, Eur. J. Inorg. Chem. 22 (2004) 4371–4374.
[86] A.I. Vovk, V.I. Kalchenko, S.A. Cherenok, V.P. Kukhar, O.V. Muzychka, M.O. Lozynsky, Org. Biomol. Chem. 2 (2004) 3162–3166.
[87] S. Cherenok, A. Vovk, I. Muravyova, A. Shivanyuk, V. Kukhar, J. Lipkowski, V. Kalchenko, Org. Lett. 8 (2006) 549–552.
[88] A.I. Vovk, L.A. Kononets, V.Y. Tanchuk, S.O. Cherenok, A.B. Drapailo, V.I. Kalchenko, V.P. Kukhar, Bioorg. Med. Chem. Lett. 20 (2010) 483–487.
[89] F.J. Steemers, H.G. Meuris, W. Verboom, D.N. Reinhoudt, E.B. van der Tol, J.W. Verhoeven, J. Org. Chem. 62 (1997) 4229–4235.
[90] M.H.B. Grote Gansey, A.S. De Haan, E.S. Bos, W. Verboom, D.N. Reinhoudt, Bioconjug. Chem. 10 (1999) 613–623.
[91] G. Montavon, U. Repine, C. Apostolidis, F. Bruchertseifer, K. Abbas, A. Morgenstern, Dalton Trans. 39 (2010) 1366–1374.
[92] K.J.C. Van Bommel, W. Verboom, R. Hulst, H. Kooijman, A.L. Spek, D.N. Reinhoudt, Inorg. Chem. 39 (2000) 4099–4106.
[93] C. Fischer, G. Sarti, A. Casnati, B. Carrettoni, I. Manet, R. Schuurman, M. Guardigli, N. Sabbatini, R. Ungaro, Chem. Eur. J. 6 (2000) 1026–1034.
[94] A. Casnati, L. Baldini, F. Sansone, R. Ungaro, N. Armaroli, D. Pompei, F. Barigelletti, Supramol. Chem. 14 (2002) 281–289.
[95] É. Tóth, A. Merbach, The Chemistry of Contrast Agents in Medical Magnetic Resonance Imaging, Wiley, Chichester, UK, 2001.
[96] E.M. Georgiev, D.M. Roundhill, Inorg. Chim. Acta 258 (1997) 93–96.
[97] L.H. Bryant Jr., A.T. Yordanov, J.J. Linnoila, M.W. Brechbiel, J.A. Frank, Angew. Chem. Int. Ed. 39 (2000) 1641–1643.
[98] S. Aime, A. Barge, M. Botta, A. Casnati, M. Fragai, C. Luchinat, R. Ungaro, Angew. Chem. Int. Ed. 40 (2001) 4737–4739.
[99] A.M. Krishnan, R. Lohrmann, R. WO96/14876, 1996.
[100] D.T. Schühle, J. Schatz, S. Laurent, L. Vander Elst, R.N. Muller, M.C.A. Stuart, J.A. Peters, Chem. Eur. J. 15 (2009) 3290–3296.
[101] D.T. Schühle, M. Polášek, I. Lukeš, T. Chauvin, É. Tóth, J. Schatz, U. Hanefeld, M.C.A. Stuart, J.A. Peters, Dalton Trans. 39 (2010) 185–191.
[102] D.T. Schühle, P. van Rijn, S. Laurent, L. Vander Elst, R.N. Muller, M.C.A. Stuart, J. Schatz, J.A. Peters, Chem. Commun. 46 (2010) 4399–4401.
[103] M. Nath, S. Pokharia, R. Yadav, Coord. Chem. Rev. 215 (2001) 99–149.
[104] A. Ali, S.J. Flora, G. Saxena, E. Kolehmainen, B. Mahieu, C.P. Rao, J. Inorg. Biochem. 100 (2006) 206–213.
[105] D.S. Kalinowski, D.R. Richardson, Pharmacol. Rev. 57 (2005) 547–583.
[106] V.S. Pires, F. Gaboriau, J. Guillon, S. Da Nascimento, A. Dassonville, G. Lescoat, V. Desplat, J. Rochette, C. Jarry, P. Sonnet, J. Enzyme Inhib. Med. Chem. 21 (2006) 261–2670.
[107] P. Rouge, V.S. Pires, F. Gaboriau, A. Dassonville-Klimpt, J. Guillon, S. Da Nascimento, J.-M. Leger, G. Lescoat, P. Sonnet, J. Enzyme Inhib. Med. Chem. 25 (2010) 216–227.
[108] L. Kelland, Nat. Rev. Cancer 7 (2007) 573–584.
[109] N.J. Wheate, G.M. Abbott, R.J. Tate, C.J. Clements, R. Edrada-Ebel, B.F. Johnston, J. Inorg. Biochem. 103 (2009) 448–454.
[110] L.F.A. Nault, C. Girardot, A. Leydier, A.W. Coleman, T. Perrottom, S. Magnard, H. Baubichon-Cortay, New J. Chem. 34 (2010) 1812–1815.
[111] A. Spagnul, C. Bouvier-Capely, G. Phan, F. Rebière, E. Fattal, Health Phys. 99 (2010) 430–434.